Eur. Phys. J. C (2024) 84:1269
https://doi.org/10.1140/epjc/s10052-024-13601-z

THE EUROPEAN PHYSICAL JOURNAL C

Regular Article

Theoretical Physics

Rips and regular future scenario with holographic dark energy: a comprehensive look

I. Brevik[1,a], **Maxim Khlopov**[2,3,4,b], **S. D. Odintsov**[5,6,c], **Alexander V. Timoshkin**[7,8,d], **Oem Trivedi**[9,e]

[1] Department of Energy and Process Engineering, Norwegian University of Science and Technology, 7491 Trondheim, Norway
[2] Research Institute of Physics, Southern Federal University, 344090 Rostov-on-Don, Russia
[3] Virtual Institute of Astroparticle Physics, 75018 Paris, France
[4] Center for Cosmoparticle Physics Cosmion, National Research Nuclear University "MEPHI", 115409 Moscow, Russia
[5] Institute of Space Sciences (ICE, CSIC), C. Can Magrans s/n, 08193 Barcelona, Spain
[6] ICREA, Passeig Luis Companys, 23, 08010 Barcelona, Spain
[7] Institute of Scientific Research and Development, Tomsk State Pedagogical University (TSPU), 634061 Tomsk, Russia
[8] Lab. for Theor. Cosmology, International Centre of Gravity and Cosmos, Tomsk State University of Control Systems and Radio Electronics (TUSUR), 634050 Tomsk, Russia
[9] International Centre for Space and Cosmology, Ahmedabad University, Ahmedabad 380009, India

Received: 10 June 2024 / Accepted: 10 November 2024
© The Author(s) 2024

Abstract Interest on the possible future scenarios the universe could have has grew substantially with breakthroughs on late-time acceleration. Holographic dark energy (HDE) presents a very interesting approach towards addressing late-time acceleration, presenting an intriguing interface of ideas from quantum gravity and cosmology. In this work we present an extensive discussion of possible late-time scenarios, focusing on rips and similar events, in a universe with holographic dark energy. We discuss these events in the realm of the generalized Nojiri–Odintsov cutoff and also for the more primitive holographic cutoffs like Hubble, particle and event horizon cutoffs. We also discuss the validity of the generalized second law of thermodynamics and various energy conditions in these regimes. Our work points towards the idea that it is not possible to have alternatives of the big rip consistently in the simpler HDE cutoffs, and shows the flexibility of the generalized HDE cutoff as well.

1 Introduction

The discovery of the Universe's late-time acceleration marked a major milestone in cosmology [1]. Following this breakthrough, substantial work has been dedicated to deciphering this expansion and literature has explored numerous approaches, including conventional methods such as the Cosmological constant [2–4], unconventional theories like Modified gravity [5–7], and models where scalar fields drive the late-time cosmic acceleration [8–13]. Quantum gravity theories, such as Braneworld cosmology in string theory, loop quantum cosmology, and asymptotically safe cosmology, have also contributed to addressing the cosmic-acceleration puzzle [14–24]. Nevertheless, inconsistencies persist, exemplified by the well-known Hubble tension, which underscores the limitations of our current understanding of the Universe and is evidenced by conflicting measurements of the Hubble constant [25–27]. Therefore, the current epoch of the Universe raises profound questions, with the potential for significant advancements in gravitational physics to enhance our understanding of cosmology.

Among the various proposed solutions for the issues of late-time acceleration is the idea of applying the holographic principle [28,29] to cosmology. This principle posits that a system's entropy is determined not by its volume but by its surface area [30]. This intriguing form of dark energy (DE) has gained interest, particularly given recent findings from DESI [31–33], which suggest that a departure from ΛCDM cannot be entirely ruled out. The initial research on holographic dark energies (HDE) by [34] suggested through a quantum field theory (QFT) approach that a short-distance cutoff is linked to a long-distance cutoff due to black hole formation constraints. Specifically, if ρ represents the quan-

[a] e-mail: iver.h.brevik@ntnu.no
[b] e-mail: khlopov@apc.in2p3.fr
[c] e-mail: odintsov@ice.csic.es
[d] e-mail: alex.timosh@rambler.ru
[e] e-mail: oem.t@ahduni.edu.in (corresponding author)

Published online: 09 December 2024

tum zero-point energy density from a short-distance cutoff, the total energy within a region of size L should not exceed the mass of a black hole of the same size, leading to the inequality $L^3\rho \leq LM_{\rm pl}^2$. The maximum allowable value for the infrared cutoff ($L_{\rm IR}$) precisely satisfies this inequality, resulting in the relation:

$$\rho = 3c^2 L_{\rm IR}^{-2}, \tag{1}$$

where c is an arbitrary parameter, and we are using $m_p = 1$ units[1]

This principle has found extensive application in cosmology, particularly in explaining the late-time dark energy era, known as holographic dark energy (HDE) (for a comprehensive review, see [35]). In this context, the infrared cutoff, $L_{\rm IR}$, is cosmologically significant and serves as the IR cutoff for a specific HDE model. Numerous studies have examined holographic dark energy from various perspectives in recent years [35–57]. Over recent decades, several alternative forms of HDE have been proposed. For example, Tsallis HDE models incorporate Tsallis' corrections to the standard Boltzmann–Gibbs entropy, resulting in the equation:

$$\rho_\Lambda = 3c^2 L^{-(4-2\sigma)} \tag{2}$$

where σ is the Tsallis parameter, assumed to be positive [58], with the simple HDE recovered in the limit $\sigma \to 1$. The Tsallis relations are also confirmed by the quantum gravity, and can lead to interesting cosmological setups. Conversely, Barrow's modification of the Bekenstein–Hawking formula led to Barrow HDE models described by the energy density:

$$\rho_\Lambda = 3c^2 L^{\Delta-2} \tag{3}$$

where Δ is the deformation parameter [59], capped at $\Delta = 1$, and the simple HDE is regained in the limit of $\Delta \to 0$. Barrow was inspired by the Covid-19 virus illustrations and he ended up showing that quantum-gravitational effects could introduce fractal features on the black-hole structure. This complex structure leads to finite volume but with infinite (or finite) area, and therefore to a deformed black-hole entropy expression which lead to the form of the HDE energy density as above. In recent times, a substantial body of literature has emerged focusing on the exploration of various types of singularities that may arise in the future evolution of the Universe. The detection of late-time acceleration has significantly propelled such investigations [60–75]. A particularly interesting class of such future events are rip scenarios, where the universe may proceed towards progressive disintegration in various capacities. An interesting question to ponder then is to ask which rip scenarios would be feasible in the vast array of holographic dark energy models. A recent work [56] addressed this in the context of HDE models with the Granda–Oliveros cutoff [38], finding that the overarching possibility is that of the big rip while its alternatives are harder to come by. In this work we would like to go even further and take into account all other possible forms of IR cutoff for HDE theories and consider the feasibility of various rip and rip-like scenarios here. We would discuss these events with the primitive HDE cutoffs of the Hubble horizon, particle horizon and event horizon types, considering these events with these cutoffs in the conventional HDE model (1), Tsallis model (2) and Barrow model (3). We would also discuss about the generality of the Nojiri–Odintsov cutoff (N–O cutoff), and how it can facilitate multiple scenarios in this case as well. In Sect. 2 we shall give a brief overview of rip scenarios and some of the methods which have been discussed in a bid to avoid them. In Sect. 3 we shall discuss the generalized Holographic dark energy paradigm with the N–O cutoff and look at how various future scenarios can be accommodated in it. In Sect. 4 we shall discuss about such future events with the Hubble horizon cutoff, while in Sects. 5 and 6 we shall discuss it for the particle and event horizon cutoffs. In Sect. 7 we shall discuss about the thermodynamic aspects and the validity of energy conditions in various scenarios, while we conclude our work in Sect. 8.

2 Rips, cosmological singularities and their avoidance procedures

An interesting variety of rip scenarios have been put forward in recent years. Even besides rip models, a rich literature on future cosmological singularities has also developed and we can summarize the rip possibilities and other singularities as follows:

- Big Rip (Type I singularity): A well-known scenario where, as $t \to t_f$ (with t_f finite), both the effective energy density and pressure density of the universe diverge, $\rho_{eff} \to \infty$, $p_{eff} \to -\infty$, and the Hubble parameter also diverges, $H \to \infty$ [76]. This results in a scenario of universal destruction, where everything in the universe undergoes progressive disintegration [76].
- Little Rip (LR): In this scenario, the density, pressure, and Hubble parameter become infinite as $t \to \infty$ [77]. In this case, all bound structures are eventually torn apart, but there is no finite-time singularity.
- Pseudo Rip (PR): Here, H increases monotonically as $t \to \infty$, but it is bounded from above by the value H_∞ so that $H \to H_\infty$ as $t \to \infty$ [78].
- Sudden singularity (Type II singularity): In the case of type II singularities, the pressure density diverges and so does the derivatives of the scalar factor from the second derivative onwards [79]. The weak and strong energy conditions hold for this singularity. Also known as quies-

[1] We would like to emphasize that we shall be using the $m_p = 1$ units throughout the paper, for the other HDEs theories as well.

cent singularities,[2] a special case of this is the big brake singularity [81].
- Big Freeze (Type III singularity): In this case, the derivative of the scale factor from the first derivative onward diverges. These were detected in generalized Chaplygin gas models [82].
- Generalized sudden singularities (Type IV singularities): These are finite time singularities with finite density and pressure instead of diverging pressure. In this case, the derivative of the scale factor diverges from a derivative higher than the second [63,83].

Note that the Little Rip and Pseudo Rip are infinite future singularities while the others are finite-time singularities.These singularities have been found and discussed in a huge array of cosmological models, ranging from simple ΛCDM models, to exotic models of all kinds like Chaplygin gas, scalar field dark energy models, modified gravity theories, Braneworld cosmologies etc. [74,75]. With such singularities being found in various models, a natural interest also grew in finding ways to avoid, delay or outright remove these singularities. An approach to mitigating or delaying singularities involves considering the effects of conformal anomalies. The impact of quantum backreaction of conformal matter on Type I, Type II, and Type III singularities was explored in [60,62,84]. Around singularity time $t = t_s$, the curvature of the universe becomes large, although the scale factor a remains finite for Type II and III singularities. Quantum corrections, which typically involve powers of curvature or higher derivative terms, become significant near the singularity.

Conformal anomalies occur due to the presence of one-loop vacuum contributions from various matter fields, breaking the conformal invariance of the matter action in the renormalized action. The trace of the energy-momentum tensor in a conformally invariant theory is zero classically, but renormalization leads to a non-zero trace, known as the conformal anomaly. The conformal anomaly can be expressed as [62]:

$$T_A = b\left(F + \frac{2}{3}\Box R\right) + b'G + b''\Box R \tag{4}$$

where T_A is the trace of the stress-energy tensor, F is the square of the 4D Weyl tensor, and G is the Gauss–Bonnet curvature invariant, defined as:

$$F = \frac{1}{3}R^2 - 2R_{ij}R^{ij} + R_{ijkl}R^{ijkl} \tag{5}$$

$$G = R^2 - 4R_{ij}R^{ij} + R_{ijkl}R^{ijkl} \tag{6}$$

The coefficients b and b' are given by:

$$b = \frac{N + 6N_{1/2} + 12N_1 + 611N_2 - 8N_{HD}}{120(4\pi)^2} \tag{7}$$

$$b' = -\frac{N + 11N_{1/2} + 62N_1 + 1411N_2 - 28N_{HD}}{360(4\pi)^2} \tag{8}$$

where N is the number of scalar fields, $N_{1/2}$ is the number of spinor fields, N_1 is the number of vector fields, N_2 (which can be 0 or 1) represents gravitons, and N_{HD} denotes higher derivative conformal scalars. Typically, $b > 0$ and $b' < 0$ for ordinary matter, except for higher derivative conformal scalars, while b'' can be arbitrary.

Quantum effects due to the conformal anomaly act as a fluid with energy density ρ_A and pressure p_A. The total energy density is $\rho_{tot} = \rho + \rho_A$. The conformal anomaly (trace anomaly) can be given by:

$$T_A = -\rho_A + 3p_A \tag{9}$$

Using the continuity equation, we have [62]:

$$T_A = -4\rho_A - \frac{\dot{\rho_A}}{H} \tag{10}$$

In standard cosmology, ρ_A can be expressed as an integral in terms of T_A:

$$\rho_A = -\frac{1}{a^4}\int a^4 H T_A dt \tag{11}$$

Furthermore, T_A can be written in terms of the Hubble parameter:

$$\begin{aligned} T_A = &-12b\dot{H}^2 + 24b'(-\dot{H}^2 + H^2\dot{H} + H^4) \\ &-(4b + 6b'')(H^{(3)} + 7H\ddot{H} + 4\dot{H}^2 + 12H^2\dot{H}) \end{aligned} \tag{12}$$

Using this, ρ_A can be derived to account for conformal anomaly effects near singularities. One can then find out that this setup can mitigate quite a few future rips and singularities. Consider the EOS being taken of the form $p = -\rho - f(\rho)$ with $f\rho) = B\rho^\beta$, where B and β are positive constants. This is a form which has been shown to be a valid cosmology to give quite a few future singularities including the big rip, and these conformal anomaly effects are enough to alleviate even the big rip in this case [60]. The conformal anomaly effects do not always work [85], however, they are nonetheless quite effective. There are other approaches to mitigating these singularities as well, one such being about considering in a modified gravity background [6,7,86]. One can even consider cosmologies with varying physical constants, like speed of light or the gravitational constant [87]. It has been shown to regularize cosmological singularities in certain scenarios [88–91]. A common theme in these approaches is that they consider ways of modifying the background gravitational theory or other fundamental essentials of standard cosmology in order to alleviate the issues of singularities. We would now like to discuss in the next section how holographic dark energy approaches this scenario, and how it can alleviate rips and other singularities in the generalized HDE scenario.

[2] This name originally appeared in contexts related to non-oscillatory singularities [80].

3 Generalized holographic dark energy and late-time scenarios

There has been a flurry of work on the paradigm of Holographic dark energy theories in recent times. This has resulted in a diversified literature where various forms of the energy density of the HDE alongside various potential cutoff scales have been discussed. The initial HDE proposals had dealt with the simple IR cutoff where the scale L was identified with

$$L \to H^{-1} \tag{13}$$

where H is the Hubble parameter, with this cutoff being regarded as the Hubble horizon cutoff. More involved cutoffs included those where the cutoff was identified with the particle Horizon

$$L_p = a \int_0^t \frac{dt}{a} \tag{14}$$

or with the future cosmological event horizon

$$L_f = a \int_a^\infty \frac{dt}{a} \tag{15}$$

These different cutoff choices, while popular, had their own set of issues as well. In the case of the Hubble horizon for example, it was found that this particular scale resulted in an equation of state approaching zero, failing to contribute significantly to the current accelerated expansion of the universe. In the particle horizon approach the equation of state parameter higher than $-\frac{1}{3}$ but the struggle of explaining the present acceleration remained as it was. In the event horizon case one was getting the desired results, although at the cost of issues with regards to causality, posing a significant obstacle to its viability.[3] Another choice which was then proposed for the HDE cutoff was the Granda–Oliveros cutoff, where one has

$$L = \left(\alpha H^2 + \beta \dot{H}\right)^{\frac{-1}{2}} \tag{16}$$

This cutoff[4] was proposed in order alleviate the issues that the former cutoffs and while it does give desired results in a large number of cases, arguably better performing than the previous cutoffs, one can still have other issues like a prominent one with regards to the classical stability of the HDE models. This comes around due to the fact that various HDE models, in all 4 cutoffs as discussed above, have been seen to have negative squared sound speeds which is indeed a worrisome feature. There are other issues where the Granda–Olvieros can, in principle, perform better than the other cutoffs as well like with regards to validity of energy conditions and the validity of the generalized second law of thermodynamics in models with these cutoffs.

A general observation one can make here is that the results in HDE scenarios become better suited given a more suitable and dynamic interplay of cosmological parameters in the cutoff scale. Another key point to note is that a prominent issue of the original holographic dark energy model [93], where the infrared cutoff was chosen as the size of the event horizon, was that the corresponding FLRW equations often do not correspond to any covariant gravity theory and even may not predict universal acceleration appropriately. With these notions in mind, one turns their attention to the generalized holographic dark energy scenario, where L is identified by the N–O given as [53]

$$L = L(L_p, \dot{L_p}, \ddot{L_p}, \ldots, L_f, \dot{L_f}, \ddot{L_f}, \ldots, H, \dot{H}, \ddot{H}, \ldots) \tag{17}$$

As is clear from (17), this cutoff scale encapsulates all the previous proposals we have discussed. All of the Hubble, particle, event and Granda–Oliveros cutoff scales turn into special cases of this generalized N–O cutoff scheme. Given the general and quite unique setup of the cutoff, it is hence of interest to study late universe events in this paradigm as well. Recently in [56] the authors showed discussed about the possibility of various rip events in quite a few HDE models with the Granda–Oliveros cutoff. The authors were able to show that the overarching possibility in such models is the Big rip, which can happen in almost any HDE model while a pseudo rip is also a real possibility in some cases. The curious feature is that the little rip occurs is virtually impossible to have in HDE scenarios with this cutoff. Given the fact that the G-O cutoff in general presents a more complete HDE scenario than the simple Hubble, particle and event horizon cases, it is indeed an interesting result. Building on this, however, one can then also ask about the possibility of various rip events in the the N–O cutoff and we would like to briefly discuss this as well.

For the moment, we shall consider the conventional HDE energy density (1) i.e. we are not considering any extended HDE scenarios like Tsallis, Barrow etc. Considering that in the very late universe, dark energy is the dominant material component one can say, without loss of generality, that $\rho_{DE} > \rho_m, \rho_r$, where ρ_m and ρ_r mean the matter and radiation energy densities, respectively. With this in mind, one can then write using the Friedmann equation

$$H^2 = \frac{\rho}{3} \sim \frac{\rho_{DE}}{3} \tag{18}$$

[3] Note that these observations are in regards to these cutoffs being used in the conventional HDE energy density setup with $\rho_{DE} \to L^{-2}$ (1), however these worries have been expressed in other HDE models with these cutoffs as well.

[4] Note that these models have also been referred to as "generalized ghost dark energy" as well [92].

while being given the cutoff (16)

$$\int_{H_i}^{H_f} \frac{\beta c^2 dH}{H^2(1-\alpha c^2)} = \frac{\beta c^2\left(\frac{1}{H_i}-\frac{1}{H_f}\right)}{1-\alpha c^2} = \int_{t_i}^{t_f} dt. \tag{19}$$

From this it is pretty clear that in the context of this HDE model with the Granda–Oliveros cutoff, only a big rip scenario can be allowed for. In general now, one can find an integral of the form [56]

$$\int_{H_i}^{H_f} \frac{dH}{g(H)} = \int_{t_i}^{t_f} dt \tag{20}$$

The above integral can come from various HDE models in the G-O cutoff paradigm, including various modifications of the simple HDE energy density. For $H_f \to \infty$, if the integral on the LHS (20) then we have $t_f \to \infty$ as well, which means that a little rip could be a possibility. Similarly if the LHS stays finite for $H_f \to \infty$ then a big rip could happen while if the integral diverges for a finite H_f then we have a pseudo rip scenario. However, the above integral can also be obtained from the generalized N–O cutoff as well and one can work through the corresponding integrals with the same conditions to talk of rips in those cases as well. Here we would like to make the case that in the generalized cutoff scale events which are "forbidden" in the G-O cutoff scale can also take place here. Consider for example a more involved form of (16), given as

$$L = (\alpha_1 H + \alpha_2 H^2 + \alpha_3 H^3 + \beta \dot{H})^{-\frac{1}{2}} \tag{21}$$

where α_1, α_2 and α_3 are constants. Note that (21) becomes the Granda–Oliveros cutoff in the limit $\alpha_1, \alpha_3 \to 0$. In this case, we have the corresponding integral on the LHS as in (20) as

$$\int_{H_i}^{H_f} \frac{dH}{-\alpha_1 H + (1-\alpha_2)H^2 - \alpha_3 H^3} = \frac{\beta}{2\alpha_1}\left[\frac{2(\alpha_2-1)\tan^{-1}\left(\frac{\alpha_2+2\alpha_3 H-1}{\sqrt{4\alpha_1\alpha_3-\alpha_2^2+2\alpha_2-1}}\right)}{\sqrt{4\alpha_1\alpha_3-\alpha_2^2+2\alpha_2-1}} + \ln\left(\frac{(\alpha_1+H(\alpha_2+\alpha_3 H-1))}{H^2}\right)\right] + \text{constant} \tag{22}$$

We see that for

$$H \to \frac{\sqrt{4\alpha_1\alpha_3-\alpha_2^2+2\alpha_2-1}-\alpha_2+1}{2\alpha_3}$$

the integral in (22) diverges, which means this is the H takes as $t_f \to \infty$. This means that in a dark energy model with monotonically increasing DE energy density, H takes a finite value at infinite times which signifies that we could have a pseudo rip on our hands here. This goes to show that even form a seemingly extended form of the G-O cutoff as in (21), which is again just yet another formulation of the N–O, can give us a pseudo rip scenario even when the form of the energy density is just of the conventional form. We may not even need to just rely on the integral approach in certain cases and can see more exact formulations as well. Consider the following form of (17) for example [36]

$$\frac{c}{L} = \frac{1}{L} = \left(1-\frac{1}{t_0 h_0}\right)\frac{1}{L_f} + \frac{2h_0}{t_0 h_1} + \frac{h_1}{t_0}\left(1-\frac{h_0^2}{h_1^2}\right)L_f \tag{23}$$

where we have henceforth set $c = 1$ (which is valid in these generalized schemes), with h_0, t_0, h_1 being constants with $h_0 > h_1$. In this case, one can use the Friedmann equation to get the Hubble parameter to be in the form

$$H(t) = \frac{h_1}{t_0\left(h_0 - h_1\tanh\left(\frac{t}{t_0}\right)\right)\cosh^2\left(\frac{t}{t_0}\right)} + h_0 - h_1\tanh\left(\frac{t}{t_0}\right) \tag{24}$$

One sees in this case as well that as $t \to \infty$, $H \to h_0 - h_1$, which is again a constant value and one sees again a situation of a pseudo rip. In this case one can also write

$$\dot{\rho} = \frac{2\rho\dot{L_f}}{H\sqrt{\Omega_d}}\left(\alpha_2 - \frac{\alpha_0}{L_f^2}\right) \tag{25}$$

where Ω_d is the fractional energy density parameter for DE. One can also find that

$$\frac{1}{L_f} = h_0 - h_1\tanh\left(\frac{t}{t_0}\right) \tag{26}$$

One can use this form of L_f in (25) and find that even other forms of cosmological singularities. Besides the Big Rip(Type I) and Big Freeze (Type III) singularities, there are other interesting future singularities that one also sees in various cosmological models, which include sudden (type II) and generalized sudden singularities (type IV), as we had discussed before. One can write using (24) that

$$\dot{H} = \frac{1}{t_0^2}\left(\frac{(h_1-h_0)(h_0+h_1)}{\left(h_0\cosh\left(\frac{t}{t_0}\right)-h_1\sinh\left(\frac{t}{t_0}\right)\right)^2} + (1-h_1 t_0)\,\text{sech}^2\left(\frac{t}{t_0}\right)\right) \tag{27}$$

$$\ddot{H} = \frac{1}{t_0^3}2\left(\frac{(h_0-h_1)(h_0+h_1)\left(h_0\sinh\left(\frac{t}{t_0}\right)-h_1\cosh\left(\frac{t}{t_0}\right)\right)}{\left(h_0\cosh\left(\frac{t}{t_0}\right)-h_1\sinh\left(\frac{t}{t_0}\right)\right)^3} + (h_1 t_0 - 1)\tanh\left(\frac{t}{t_0}\right)\text{sech}^2\left(\frac{t}{t_0}\right)\right) \tag{28}$$

We note interestingly that for no values of t, either finite or infinite, does the Hubble parameter or its derivatives diverge in the above cases. Furthermore, the expressions for the pressure and the energy density, which we do not reproduce here owing to their length, show the same behaviour. This shows that even type II and type IV singularities do not occur for this cutoff choice. Another example of a N–O cutoff is

$$L = (\beta \dot{H}^2)^{-\frac{1}{2}} \tag{29}$$

Using this form of the cutoff, we end up with the Hubble parameter as

$$H(t) = H_0 e^{\frac{t-t_0}{\sqrt{\beta}}} \tag{30}$$

This form of the cutoff can accommodate a Little rip scenario as H diverges here at infinite times. The reason we have considered these cases here is in order to have a gauge on whether or not the more generalized HDE cutoff can provide us with more flexibility in allowing for more late-time events when compared with the G-O cutoff. It indeed seems to be the case here, as we have seen with the cutoffs in (21), (23) and (29), and how they could naturally allow for pseudo or little rip scenarios even with the conventional HDE energy density (1). The rip possibilities one can ponder with the N–O cutoffs in extended HDE models like Tsallis, Barrow, Kaniadakis etc. would then be even more interesting to study. It is so as one can even be looking at the possibility that, given certain parameter ranges for the free parameters of these regimes, all three of these rip scenarios could be allowed for or avoided as well in the N–O scheme. This reinforces the point which was briefly mentioned in [56], which was about the possibility of the N–O cutoff in general representing the most viable way to have various late time scenarios. We can make a comment in general, based on the discussions of the cutoffs above. Consider depicting two kinds of generalized N–O cutoffs, one being the "Hubble type"

$$L = L(H, \dot{H}, \ddot{H} \ldots) \tag{31}$$

The other being the "P–E type"

$$L = L(L_p, \dot{L_p}, \ddot{L_p} \ldots, L_f, \dot{L_f}, \ddot{L_f} \ldots) \tag{32}$$

One would realize that the Hubble type (31) encapsulate the Hubble horizon (13) and the G-O cutoff (16) as special cases while the P–E type[5] encapsulates all possible cases with the particle horizon (14) and event horizon (15) cutoffs. Of course, both these formulations are just ways to rephrase the N–O cutoff (17) but it is important to make the distinction here with regards to how rips and singularities come by. In general we would like to comment that one would observe models with cutoffs of the Hubble type (31), like (21)–(29), more easily produce scenarios with rips, singularities and similar futures, given the more direct correspondence of $\rho \rightarrow f(H)$ in that case. Such a correspondence leads to cases where any blow ups in H would lead to blow ups in the densities as well, either in finite or infinite time and it would be more difficult to avoid rips and singularities in these cases. Furthermore, as mentioned before, it could very well be the case that if one considers more extended forms of the energy density (1) then the free parameters associated with the models could define ranges in their parameter space where rips and similar events could both be accommodated and avoided, but strictly speaking from the conventional HDE point of view the Hubble type cutoffs would be more difficult in terms of avoiding such blowups. On the other hand, the cutoffs of the P–E type (32) like (32) would lead to more non-singular and rip free universes. Indeed it has well known that HDE models with simple particle or event horizon cutoffs readily allow for big rip scenarios, but our comment concerns cases where one considers general functions of these cutoffs as in (32). One can say that eventually the correspondence between $\rho \rightarrow f(H)$ would stay in both cutoff bifurcations, but differences come about more clearly by how the DE energy density $\dot{\rho}$ evolves in cases of the Hubble types and of the P–E type. So in general one may observe that cosmologies with N–O cutoff of the form (32) are more non-singular than those of the form (31).

But going a step back, one is left to wonder whether if the GO cutoff is not able to support various ends of the universe, could the more simple cutoffs do? One can indeed argue that in general we would not want to have rips etc. in the universe, but it has already been discussed frequently in the literature that big rips can occur in various HDE models so it is natural to ask whether alternatives of the big rip and alike events can also be consistently plausible too. Another way to study these late-time events would be by utilizing the ansatz' for these scenarios, and using them to find the forms of relevant observational and theoretical parameters to ascertain the consistency of these events in various models. We would like to now employ this approach to study about the status quo of various late time events with the Hubble, Particle and Event horizon cutoff schemes. In order to make the analysis more extensive, we shall also consider the Tsallis and Barrow models alongside the conventional HDE model in our work, which in total provides us with 9 models (prospectively) to look at. In the subsequent sections we would be discussing about various subtleties of rips and similar events in such models and will try to gauge the flexibility of the simpler cutoffs in addressing various late-time events in the universe.

[5] By "P–E" we aim to acronymize the Particle and Event horizon type into a single phrase, as this cutoff represents all possible combinations of these scales.

4 Future events with Hubble horizon cutoff

In all the ensuing work, we shall consider an interacting dark sector. One can explore an interaction between dark energy and dark matter by incorporating the following continuity equations:

$$\dot{\rho}_\Lambda + 3H\rho_\Lambda(1+w_\Lambda) = -Q \tag{33}$$
$$\dot{\rho}_m + 3H\rho_m(1+w_m) = Q \tag{34}$$

In this context, ρ_Λ and ρ_m denote the energy densities of dark energy and dark matter, respectively. The symbol w_Λ stands for the equation of state parameter for dark energy, while w_m represents the equation of state parameter for dark matter. The interaction between these two components is described by the term Q. It is important to specify here that the sign infront of Q in RHS in the above equations specifies the kind of interaction in the dark sector, with -Q on the RHS in (33) and +Q on the RHS of (34) showing that we consider a scenario where gradually ρ_m is decaying into ρ_d. If the signs were flipped in the continuity equations above, then the reverse decay from DE to DM would instead be seen.

To simplify our analysis, we focus exclusively on the contributions of dark energy and dark matter to cosmology. The interaction term Q can be expressed in either linear or nonlinear forms. Examples include:

$$Q = 3Hb(\rho_\Lambda + \rho_m) \tag{35}$$
$$Q = 3Hb\frac{\rho_\Lambda^2}{\rho_\Lambda\rho_m} \tag{36}$$

In these equations, b is a coefficient that determines the strength of the interaction. The different linear and nonlinear forms of Q allow for an exploration of various dynamics within the interacting dark sectors. Before considering any specific ansatz, it is crucial to perform some general analysis that is independent of any particular ansatz. Additionally, we define the fractional energy densities for dark energy (DE) and dark matter (DM) as follows:

$$\Omega_\Lambda = \frac{\rho_\Lambda}{3H^2} \tag{37}$$
$$\Omega_m = \frac{\rho_m}{3H^2} \tag{38}$$

Here, ρ_Λ is dependent on the specific model of holographic dark energy (HDE) chosen. We shall employ various ansatz' here for the Hubble parameter to study the little rip and pseudo rip scenarios (see [94]) with a little rip ansatz being

$$H(t) = H_0\exp(\lambda t) \tag{39}$$

While another variant for the little rip ansatz is

$$H(t) = H_0\exp(C\exp(\lambda t)) \tag{40}$$

The ansatz for the Pseudo rip can be given as

$$H(t) = H_0 - H_1\exp(-\lambda t) \tag{41}$$

where C, H_0, H_1 and λ are positive constants with $H_0 > H_1$. While these ansatz' are generally applicable, in [95] it was studied how the ansatz should be developed for the particular case of Braneworld cosmologies. In such a scenario we have, the ansatz for the case of a Little rip, asymptotic dS (Pseudo rip) and Big Freeze in the scenario of a Braneworld background are given as,

$$a(t) = a_0\exp\left[\frac{\lambda_b}{3\alpha^2}\cosh\left(\sqrt{\frac{3\alpha^3}{2\lambda_b}}t\right)\right] \tag{42}$$
$$a(t) = a_0\exp\left[-\frac{\beta^2}{2}\left[\frac{1}{\cos\eta_0} - \sqrt{1+\left(\tan\eta_0 + \frac{\sqrt{\alpha}}{\beta}t\right)^2}\right]\right] \tag{43}$$
$$a(t) = a_f\exp\left[-\frac{\lambda_b}{3\alpha^2}\left(1-\frac{3\alpha^3t^2}{2\lambda_b}\right)^{1/2}\right] \tag{44}$$

where a_0, a_f, α are positive constants while λ_b is the brane tension. In the case of the Asymptotic dS (43) β and η_0 are also positive constants, with β being in terms of λ_b and α. Also it is worth noting that the Little rip (42) and Big Freeze (44) cases are possible with positive brane tension $\lambda_b > 0$ while the asymptotic dS case occurs with a negative brane tension $\lambda_b < 0$.

We start off with the Hubble horizon cutoff where we have

$$L \to H^{-1}$$

To start our analysis consider the usual HDE model, (1) from where we can write

$$\dot{\rho} = -2\rho\frac{\dot{L}}{L} \tag{45}$$

In the case of the cutoff (13), we have

$$-\frac{\dot{L}}{L} = \frac{\dot{H}}{H} \tag{46}$$

From which we end up with the expression

$$\dot{\rho} = \frac{2\dot{H}\rho}{H} \tag{47}$$

We can then use it in the continuity equation (33) to get the equation of state parameter for dark energy as

$$w = -1 - \frac{1}{3H\Omega_d}\left(\frac{Q}{3H^2} + \frac{2\dot{H}\Omega_d}{H}\right) \tag{48}$$

Similarly for the case of the Tsallis paradigm with (2), we end up with

$$\dot{\rho} = \frac{(4-2\sigma)\dot{H}\rho}{H} \tag{49}$$
$$w = -1 - \frac{1}{3H\Omega_d}\left(\frac{Q}{3H^2} + \frac{(4-2\sigma)\dot{H}\Omega_d}{H}\right) \tag{50}$$

While in the Barrow case with (3) We have

$$\dot{\rho} = \frac{(2-\Delta)\dot{H}\rho}{H} \tag{51}$$

$$w = -1 - \frac{1}{3H\Omega_d}\left(\frac{Q}{3H^2} + \frac{(2-\Delta)\dot{H}\Omega_d}{H}\right) \tag{52}$$

We can now perform some plots in this regard. Firstly we consider the ansatz (39) and we plot the EOS parameter and squared sound speed, given by

$$v_s^2 = w + \frac{\dot{w}\rho}{\dot{\rho}} \tag{53}$$

In Fig. 1 we have plotted the EOS parameter and squared sound speed for both linear and nonlinear interactions in the ansatz (39)[6]. As is seen in Fig. 1, the EOS parameter for the first ansatz in the Hubble horizon cutoff is hovering around realistic values and asymptotes to -1 as in the case of usual rips. However, the squared sound speed is always negative and so there is no classical stability for the scenario. We also note that the results are the same for both linear and nonlinear regimes, which is a theme we observed for all the cases which we shall discuss from here onwards. Thereby we have only shown the plots for the linear interactions in the below cases as the plots have been seen to be almost the same in both linear and nonlinear regimes in all cases.

In Fig. 2 we have plotted for the second LR ansatz (40) and PR (41). What is seen again is that the EOS parameter asymptotes to -1 in both cases and the evolution of the EOS parameter is around acceptable values but the squared sound speed is again completely negative. This trend stays the same for the case of the nonlinear case too, which is why we haven't shown the plot for that case.

In Fig. 3 we have now plotted for the EOS parameter and squared sound speed in LR (42), Big Freeze (44) and asymptotic dS (43) again only in the linear regime for reasons mentioned above. We see that the Little rip and Asymptotic dS cases show acceptable evolution of the w parameter but peculiar behaviour is seen in the case of Big Freeze. In all these cases, again, there persists classical instability. From here we can conclude that none of the rip or rip-like events can be viable in the Hubble horizon cutoff given the conventional DE model.

In Fig. 4 we have plotted for the EOS parameter and squared sound speed in both LR ansatz and PR in the case of the Tsallis paradigm. We have plotted for the whole spectrum of the Tsallis parameter values to tack in generality. We see that the EOS parameter again asymptotes around -1 and has acceptable behaviour but even the Tsallis case is riddled with instabilities for all ranges of the free parameter.

In Fig. 5 we have plotted similarly for the Tsallis case in the Braneworld for LR, Big Freeze and asymptotic dS. We again see that there is some peculiar evolution in the case of the big freeze in its EOS but the EOS evolution for LR and asymptotic dS seem fine. Again there are instabilities, even though the Big Freeze case starts off slightly positive with regards to its squared sound speed but becomes negative again.

We then plotted for the same in Fig. 6 for the Barrow model with for the both LR ansatz and PR. We again see that the EOS parameter has acceptable evolution but the squared sound speed is negative in all cases which again shows instabilities.

In the case of the Barrow model with a Braneworld, we have plotted for the LR, Big Freeze and Asymptotic dS cases in Fig. 7. We see that the trend is similar to the usual non Barrow case even for all ranges of the deformation parameter and again there is no stability. So we would like to conclude from here that these rip and rip-like events are not viable even in Tsallis and Barrow in the Hubble horizon cutoff.

5 Future events with particle horizon cutoff

In the case of the particle horizon cutoff, we have

$$\frac{\dot{L}}{L} = \left(H + \frac{1}{L}\right)$$

Now using this, we can write

$$\dot{\rho} = -2\rho H\left(1 + \frac{\sqrt{\Omega_d}}{c}\right) \tag{54}$$

From this expression itself we can come to a very strong conclusion. For any rip event, either big rip, little rip, pseudo rip etc. we need the energy density of DE to be monotonically increasing but in this case it is completely evident that the energy density is monotonically decreasing. Hence in the particle horizon cutoff with the usual DE model, we cannot have any rip scenario occurring. Similarly in the case of the Barrow model with the particle horizon cutoff we have

$$\dot{\rho} = -(2-\Delta)\rho H\left(1 + \frac{\sqrt{\Omega_d}}{c}\right) \tag{55}$$

We again see that the energy density will be monotonically decreasing in this case as well, as $\Delta \leq 1$. In the case of the Tsallis model we have

$$\dot{\rho} = -(4-2\sigma)\rho H\left(1 + \frac{\sqrt{\Omega_d}}{c}\right) \tag{56}$$

In the case of the Tsallis model there could be a possibility energy density could be monotonically increasing when $\sigma > 2$ and so rips may be possible.

[6] For all the plots, here and thereafter, we have taken the following values for all the parameters in all the 6 ansatz mentioned above: $\Omega_d = 0.69$, $\Omega_m = 0.258$, $\alpha = 2$, $a_0 = 1$,$a_f = 1$, $b = 0.03$, $\beta = 2$, $c = 0.4$, $H_0 = 1$, $H_1 = 0.8$, $\lambda = 2$ and $\eta_0 = 4$. These parameters have been taken with the above values to be consistent with observational bounds and also with theoretical requirements on the same.

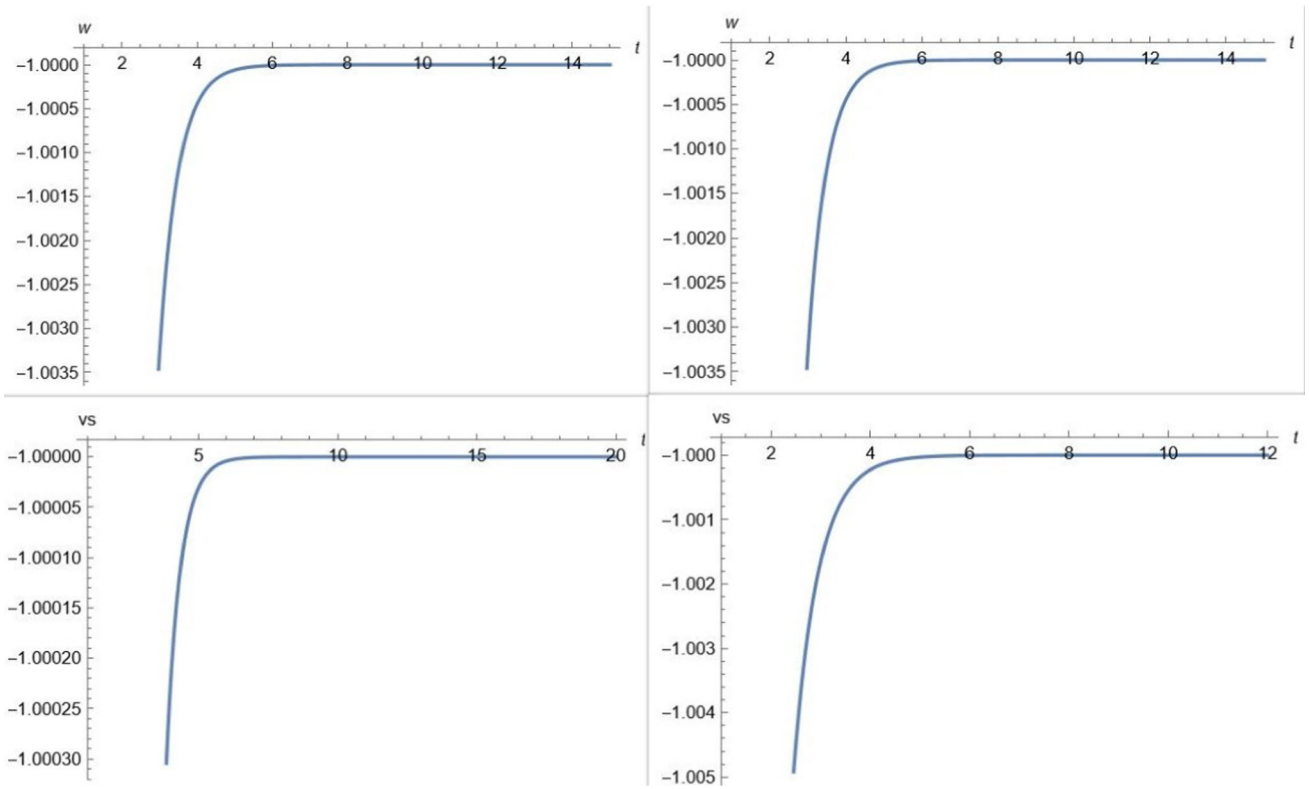


Fig. 1 Plots of the dark energy EOS parameter and squared sound speed for first LR ansatz, for both linear and nonlinear regimes for the Hubble horizon case. The upper panel shows the EOS parameter and the lower panel shows the squared sound speed, going from linear to nonlinear regimes from left to right

In Fig. 8 we have plotted for both LR ansatz and PR as we had discussed before, but for Tsallis models with particle horizon cutoff with $\sigma > 2$. Again, there is no difference in the plots and their conclusions in the linear and non-linear interaction cases. We see that similar to the cases as of before, the squared sound speed remains negative in all cases, while for larger values of σ, even the equation of state parameter touches an unrealistic range for LR as well, while it is certainly true for all range in PR.

In Fig. 9 we have plotted for the LR, asmyptotic dS and Big Freeze cases in a BraneWE again see that there is not much hope for classical stability even in these cases, while the EOS parameter is fine lower values of σ for LR and asymptotic dS case, for the Big Freeze even that is beyond an acceptable range.

6 Future events with event horizon cutoff

In the case of the event horizon, we have the following in the usual HDE model

$$\dot{\rho} = 2\rho\left(\left(\frac{\Omega_d H^2}{c^2}\right)^{\frac{1}{2}} - H\right) \tag{57}$$

The EOS parameter is

$$w = -1 - \frac{1}{3H\Omega_d}\left[(2)\Omega_d\left(\left(\frac{\Omega_d H^2}{c^2}\right)^{\frac{1}{2}} - H\right) - \frac{Q}{3H^2}\right] \tag{58}$$

While in the Tsallis model

$$\dot{\rho} = (4-2\sigma)\rho\left(\left(\frac{\Omega_d H^2}{c^2}\right)^{\frac{1}{4-2\sigma}} - H\right) \tag{59}$$

$$w = -1 - \frac{1}{3H\Omega_d}\left[(4-2\sigma)\Omega_d\left(\left(\frac{\Omega_d H^2}{c^2}\right)^{\frac{1}{4-2\sigma}} - H\right) - \frac{Q}{3H^2}\right] \tag{60}$$

And for the Barrow model, we have

$$\dot{\rho} = (2-\Delta)\rho\left(\left(\frac{\Omega_d H^2}{c^2}\right)^{\frac{1}{2-\Delta}} - H\right) \tag{61}$$

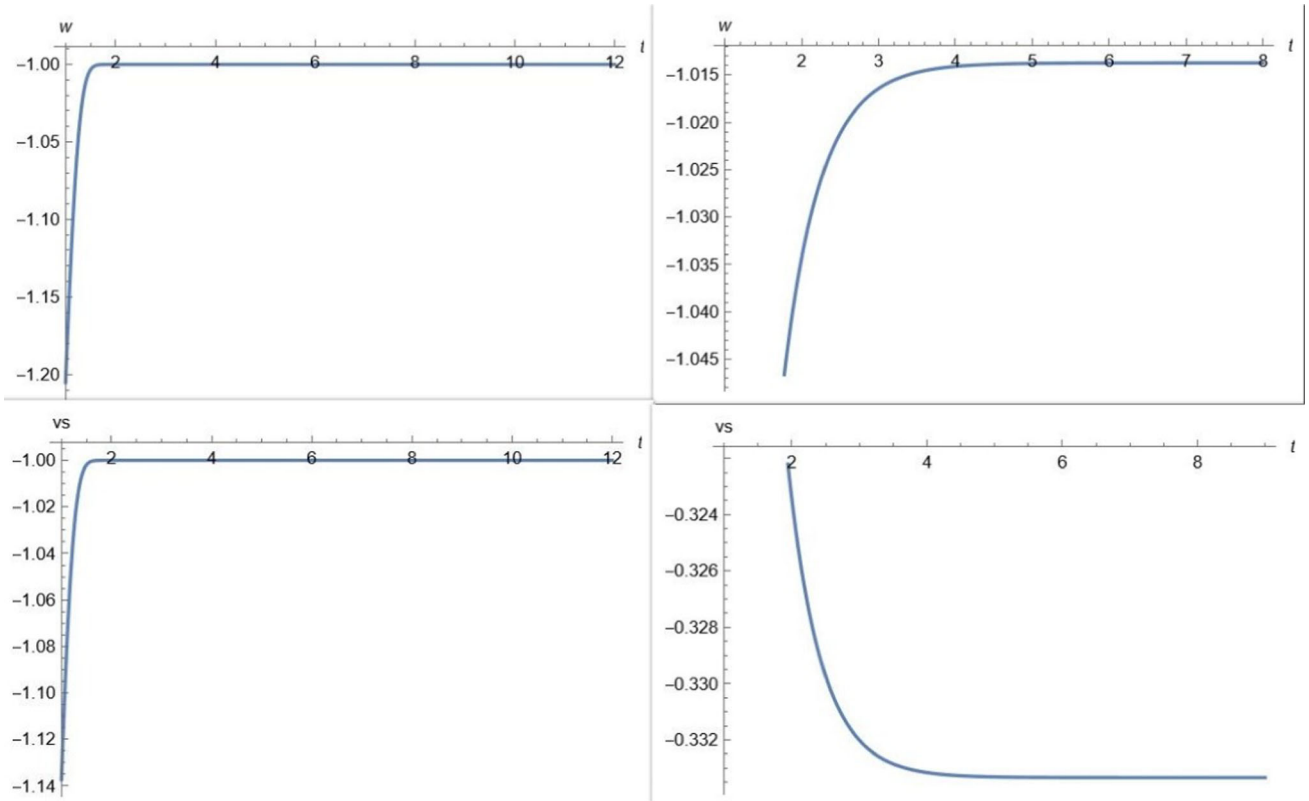


Fig. 2 Plots of the dark energy EOS parameter and squared sound speed for second LR ansatz and PR. The upper panel shows the EOS parameter and the lower panel shows the squared sound speed, going from LR to PR from left to right in the linear interaction regime

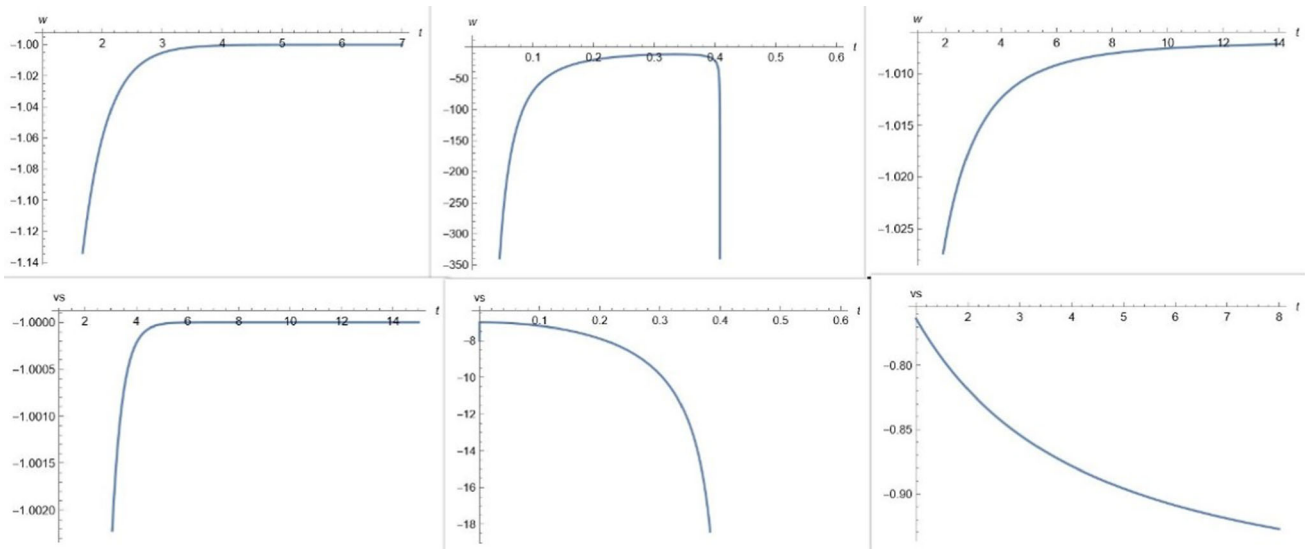


Fig. 3 Plots of the dark energy EOS parameter and squared sound speed for LR, Big Freeze and Asymptotic dS scenarios in the Braneworld for the Hubble horizon case. The upper panel shows the EOS parameter and the lower panel shows the squared sound speed, going from LR to Big Freeze to Asymptotic dS from left to right, in the linear interaction regime

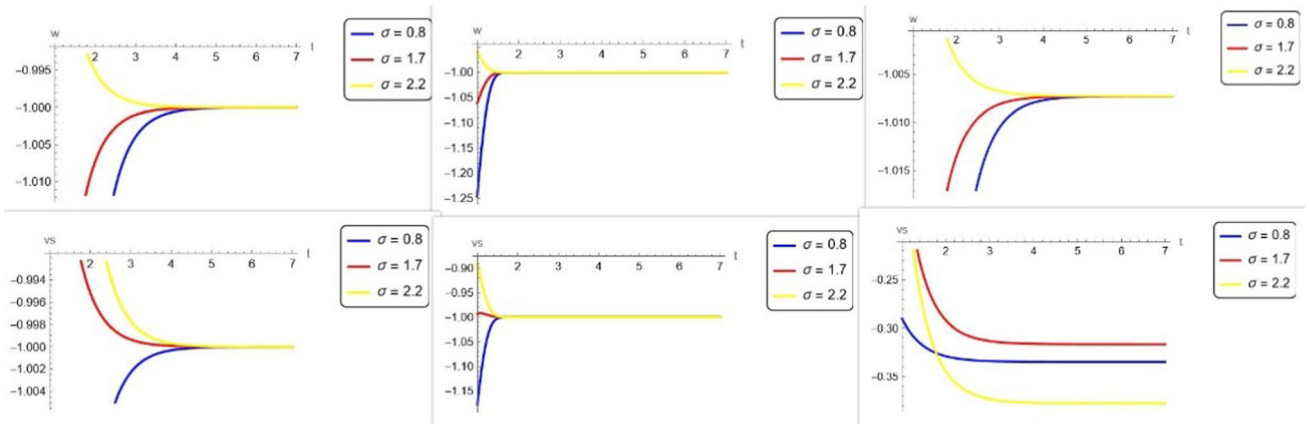


Fig. 4 Plots of the dark energy EOS parameter and squared sound speed for both LR ansatz and PR in the Tsallis paradigm for various values of the Tsallis parameter for the Hubble horizon case. The upper panel shows the EOS parameter and the lower panel shows the squared sound speed, going from LR 1 to LR 2 to PR from left to right, in the linear interaction regime

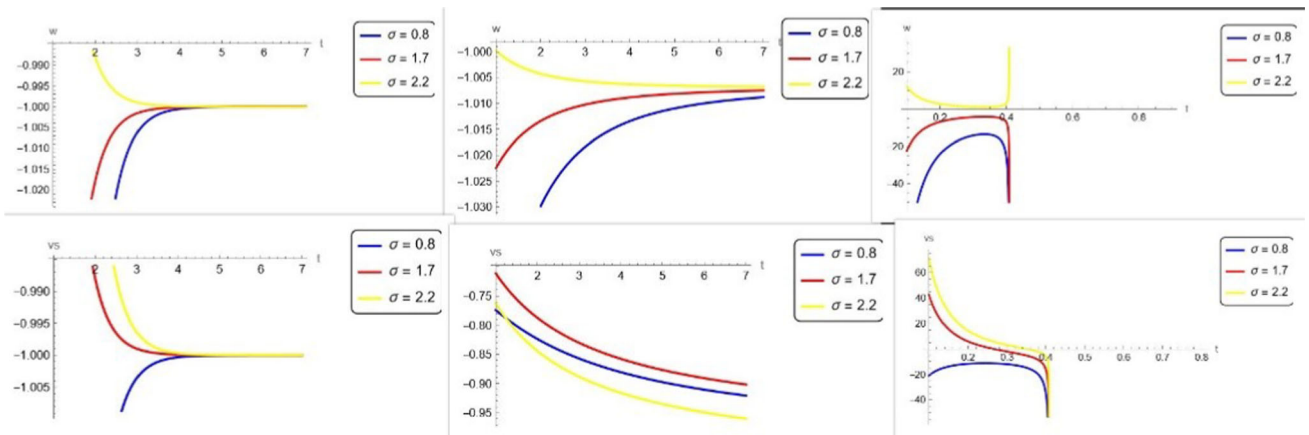


Fig. 5 Plots of the dark energy EOS parameter and squared sound speed for LR, Big Freeze and Asymptotic dS scenarios in the Braneworld in the Tsallis case for the Hubble horizon case. The upper panel shows the EOS parameter and the lower panel shows the squared sound speed, going from LR to Asymptotic dS to Big Freeze from left to right, in the linear interaction regime

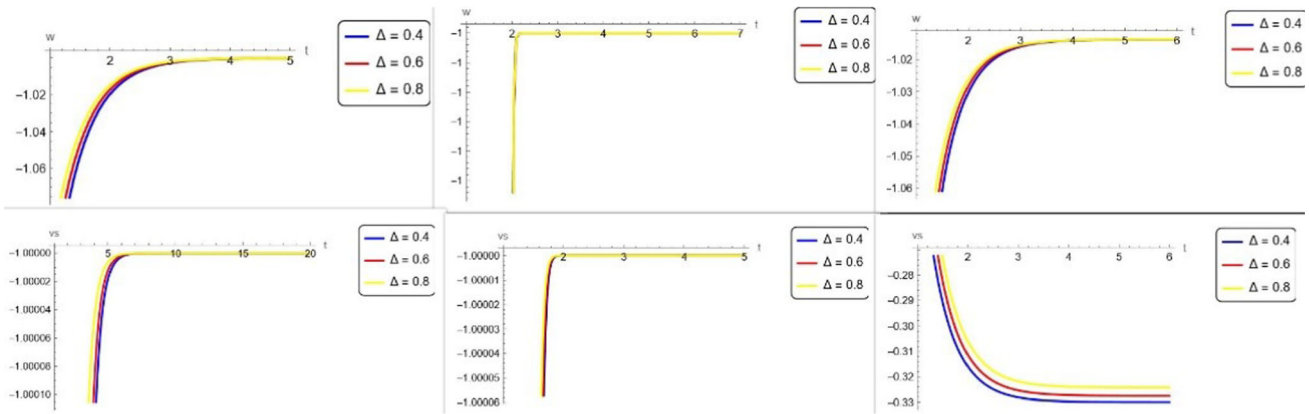


Fig. 6 Plots of the dark energy EOS parameter and squared sound speed for both LR ansatz and PR in the Tsallis paradigm for various values of the Tsallis parameter for the Hubble horizon case. The upper panel shows the EOS parameter and the lower panel shows the squared sound speed, going from LR 1 to LR 2 to PR from left to right, in the linear interaction regime

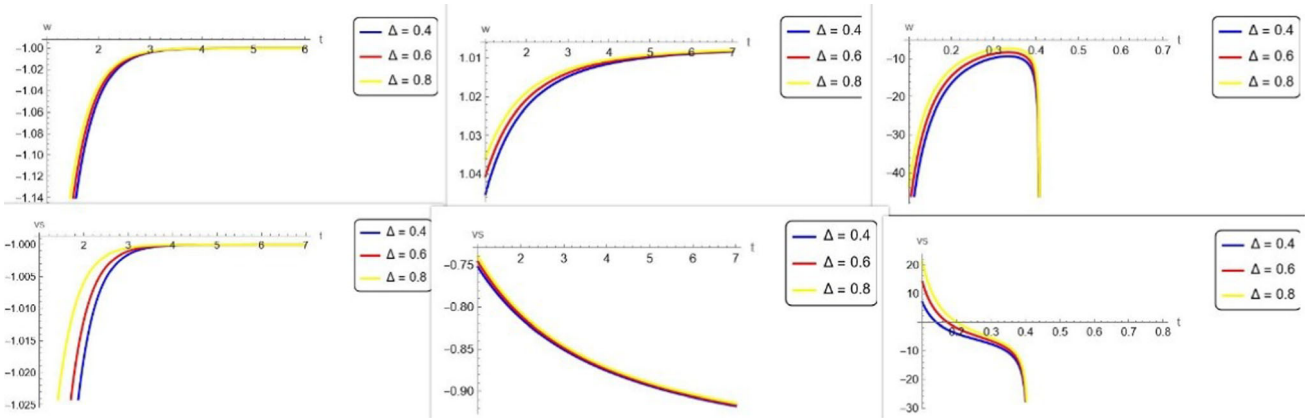


Fig. 7 Plots of the dark energy EOS parameter and squared sound speed for LR, Big Freeze and Asymptotic dS scenarios in the Braneworld in the Barrow case for the Hubble horizon case. The upper panel shows the EOS parameter and the lower panel shows the squared sound speed, going from LR to Asymptotic dS to Big Freeze from left to right, in the linear interaction regime

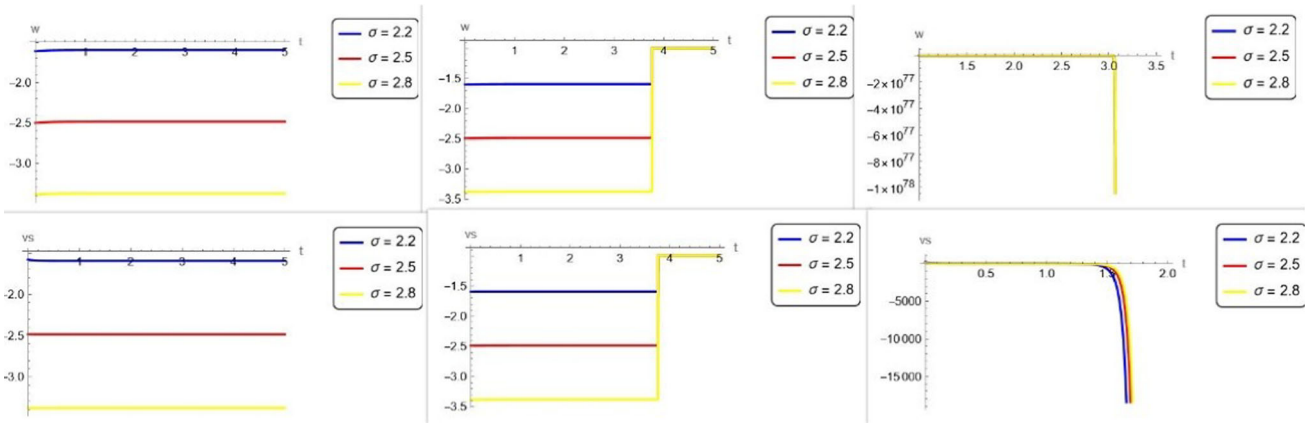


Fig. 8 Plots of the dark energy EOS parameter and squared sound speed for both LR ansatz and for PR with particle horizon case. The upper panel shows the EOS parameter and the lower panel shows the squared sound speed, going from linear to nonlinear regimes from left to right

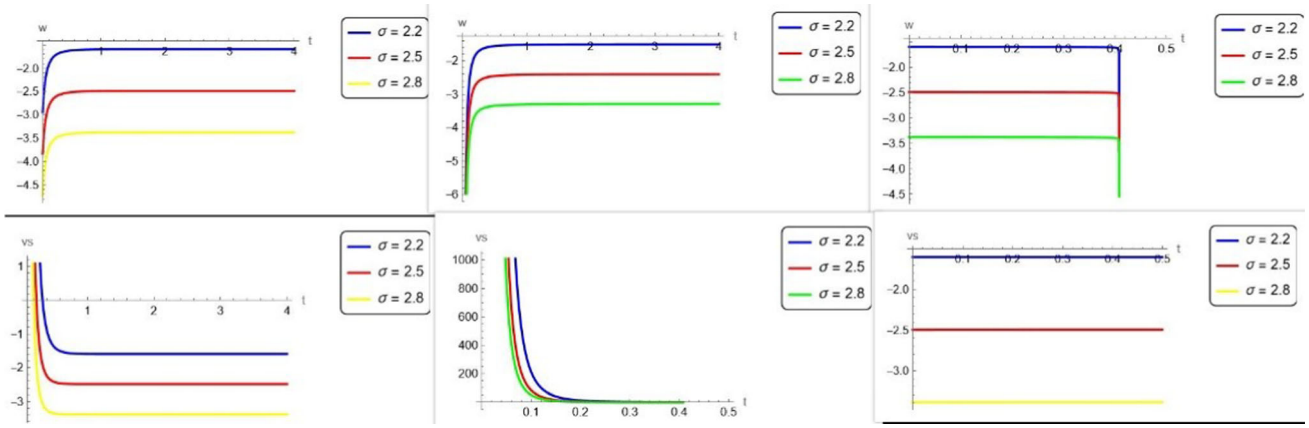


Fig. 9 Plots of the dark energy EOS parameter and squared sound speed for both LR ansatz and for PR with particle horizon case. The upper panel shows the EOS parameter and the lower panel shows the squared sound speed, going from linear to nonlinear regimes from left to right

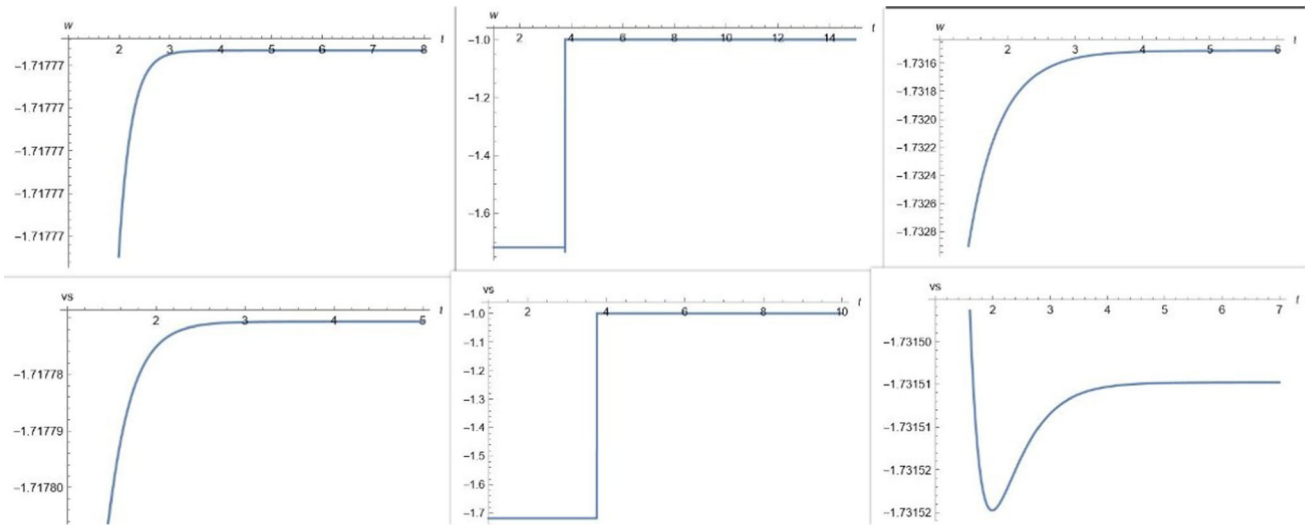


Fig. 10 Plots of the dark energy EOS parameter and squared sound speed for both LR ansatz and PR. The upper panel shows the EOS parameter and the lower panel shows the squared sound speed, going from LR 1 to LR 2 to PR from left to right, in the linear interaction regime

$$w = -1 - \frac{1}{3H\Omega_d}\left[(2-\Delta)\Omega_d\left(\left(\frac{\Omega_d H^2}{c^2}\right)^{\frac{1}{2-\Delta}} - H\right) - \frac{Q}{3H^2}\right] \quad (62)$$

In Fig. 10 we have plotted for both LR ansatz and PR for the case of the event horizon cutoff in the conventional HDE model. What one sees is a recurring pattern again, namely that the squared sound speed is negative while the EOS parameter hovers around viable values.

In Fig. 11 we have plotted for the Braneworld case for the same and we again see that there is not much hope for viable scenarios. The Big Freeze case initially produces positive squared sond speed values which eventually become negative again.

In the Barrow case for both the LR ansatz and PR as in Fig. 12, we see that the first LR unrealistic values for both w and the squared sound speed parameter as well. The case of the PR also produces overtly negative values for both the squared sound speed and EOS parameters, while the second LR seemingly gives values of the squared sound speed close to 0 but it is still negative.

In Fig. 13 we see that the Barrow model in the Braneworld also suffers from similar issues for all future events. There is no hope for stability and even the evolution of the dark energy EOS parameter is seemingly going off course for various values of the free parameter.

In Fig. 14 we see that for the case of the first LR variant, there is unrealistic evolution for both the EOS parameter and the squared sound speed parameter as well. The second LR variant shows very erratic behaviour but is closer to acceptable values for the EOS parameter however for the squared sound speed parameter it is still negative. For the PR case the story still remains the same and we again have no scenario where there is even a slight hope of stability as well.

In Fig. 15, we have plotted the dark energy EOS parameter and the squared sound speed for various values of the Tsallis parameter in the linear interaction for the Little rip scenario and we clearly see that while the squared sound speed seems to be in acceptable region (~ 0), the EOS parameter taking values ~ 0 is quite alarming and shows unrealistic values of the parameter. Exactly similar trend is seen when one plots for the same scenario in the non-linear model, as seen in Fig. 16.

When one discusses the Big Freeze singularity in the linear interaction as in Fig. 17, we see again that the EOS parameter takes values ~ 0 while squared sound speed shows values slightly below 0 or ~ 0 for various ranges of the Tsallis parameter.

Discussing the same in the non linear interaction in Fig. 18, we see that the EOS parameter is still acting the same but the squared sound speed now shows jumps and takes on absurdly negative or positive values, which are both not acceptable.

When one discusses the asymptotic dS case however, we do see some viable results. As plotted for the linear interaction case in Fig. 19, we see that for high values of σ, preferably $\sigma > 2.5$, the EOS parameter is in acceptable regions hovering around realistic negative values while at the same time, the squared sound speed maintains very small positive values close to 0.

When one considers the non-linear interaction in this scenario as in Fig. 20, we see that smaller values of σ, in the region $1.5 < \sigma < 2$ produce viable values of the EOS parameter but all models for all ranges of σ do not lead to viable sound speeds as they hover around the value of -1 only.

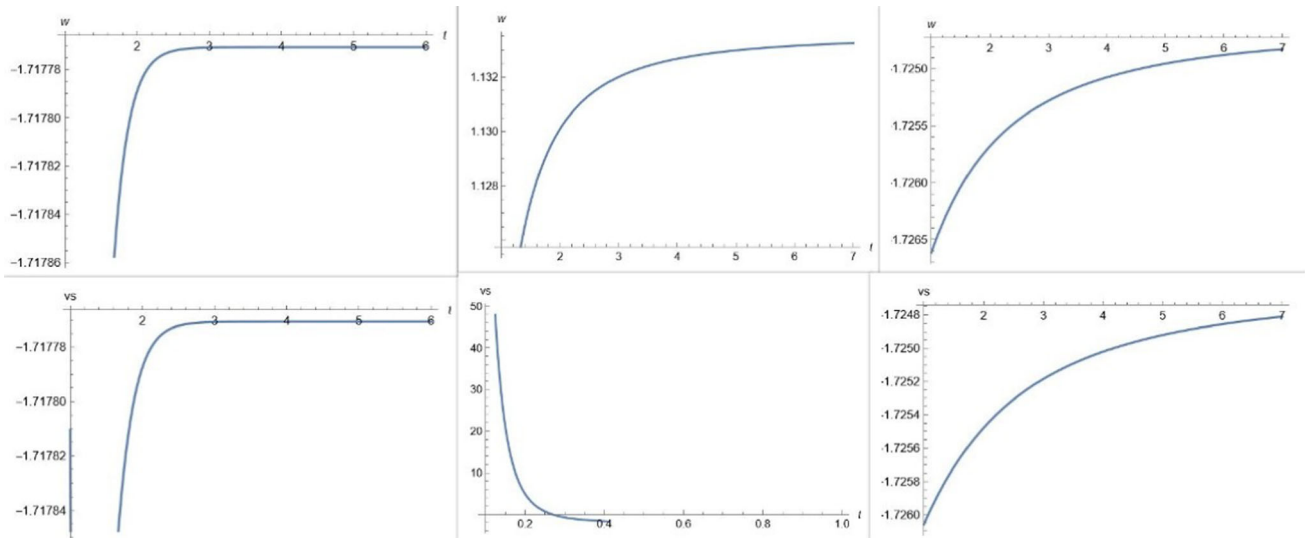


Fig. 11 Plots of the dark energy EOS parameter and squared sound speed for LR, Big Freeze and asymptotic dS. The upper panel shows the EOS parameter and the lower panel shows the squared sound speed, going from LR to Big Freeze to asymptotic dS from left to right, in the linear interaction regime

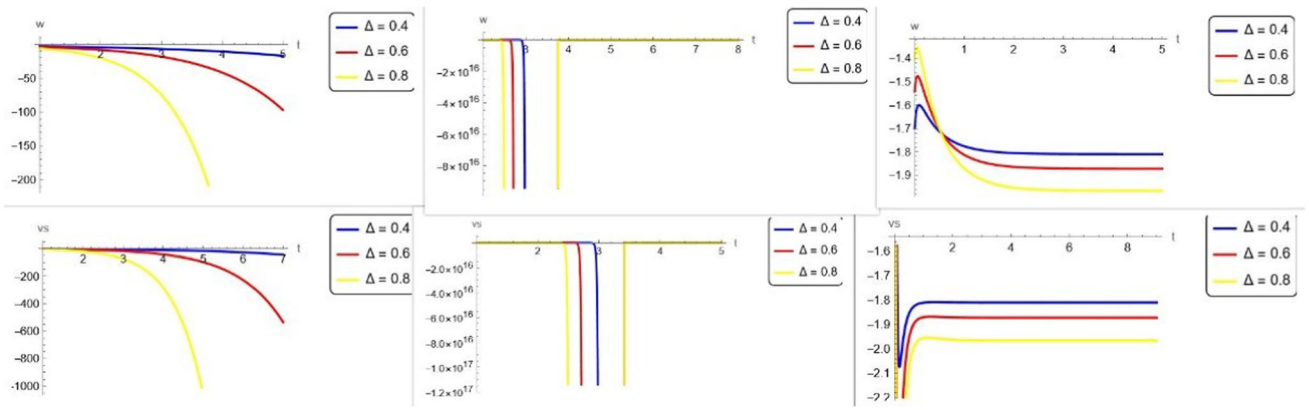


Fig. 12 Plots of the dark energy EOS parameter and squared sound speed for both LR ansatz and PR in the Barrow paradigm. The upper panel shows the EOS parameter and the lower panel shows the squared sound speed, going from LR 1 to LR 2 to PR from left to right, in the linear interaction regime

So one sees that from all these rip scenarios available, the only one which is looking viable as of now is the Asymptotic dS scenario with linear interaction for high values of the Tsallis parameter. An interesting thing to note in the Tsallis cases is that there is at least some degree of difference in behaviours in linear and nonlinear interaction regimes in the behaviour of some of the scenarios.

7 Thermodynamics and energy conditions

It is also important to address another aspect that could help ensure the consistency of holographic dark energy models, namely thermodynamics. The thermodynamic implications, especially the validity of holographic dark energy models concerning the generalized second law of thermodynamics, were recently examined in [96]. It is well known that the thermodynamic analysis of gravitational theories offers a fascinating interface with cosmology. The thermodynamic properties that hold for a black hole are equally applicable to a cosmological horizon. Moreover, the first law of thermodynamics, which holds at a black hole horizon, can also be derived from the first Friedmann equation in the FLRW universe when the universe is bounded by an apparent horizon. This provides strong motivation to select the apparent horizon as the cosmological horizon to examine the thermodynamic properties of any cosmological model.

Motivated by these arguments, we consider the universe as a thermodynamic system bounded by the cosmological

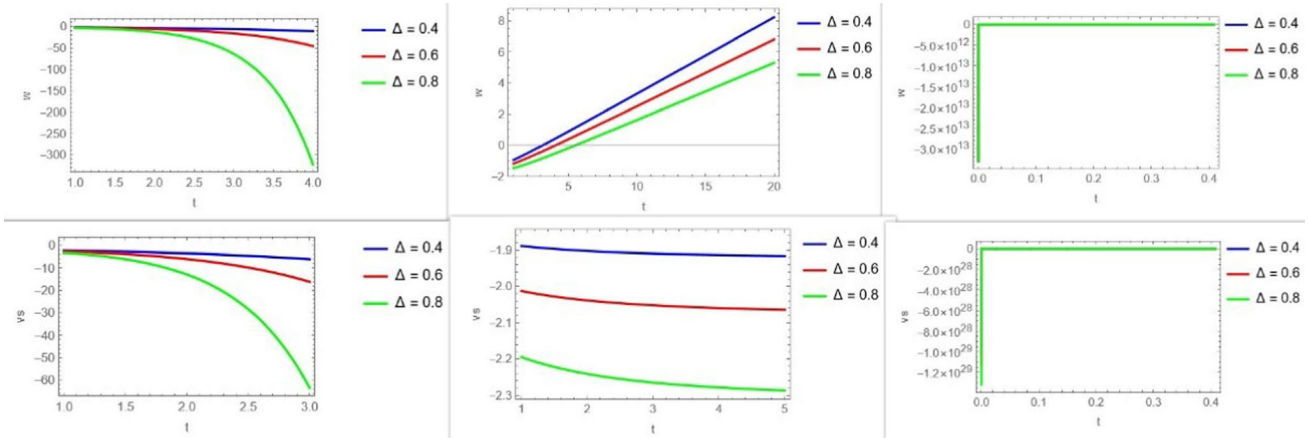


Fig. 13 Plots of the dark energy EOS parameter and squared sound speed for LR, Big Freeze and asymptotic dS in the Barrow paradigm. The upper panel shows the EOS parameter and the lower panel shows the squared sound speed, going from LR to Big Freeze to asymptotic dS from left to right, in the linear interaction regime

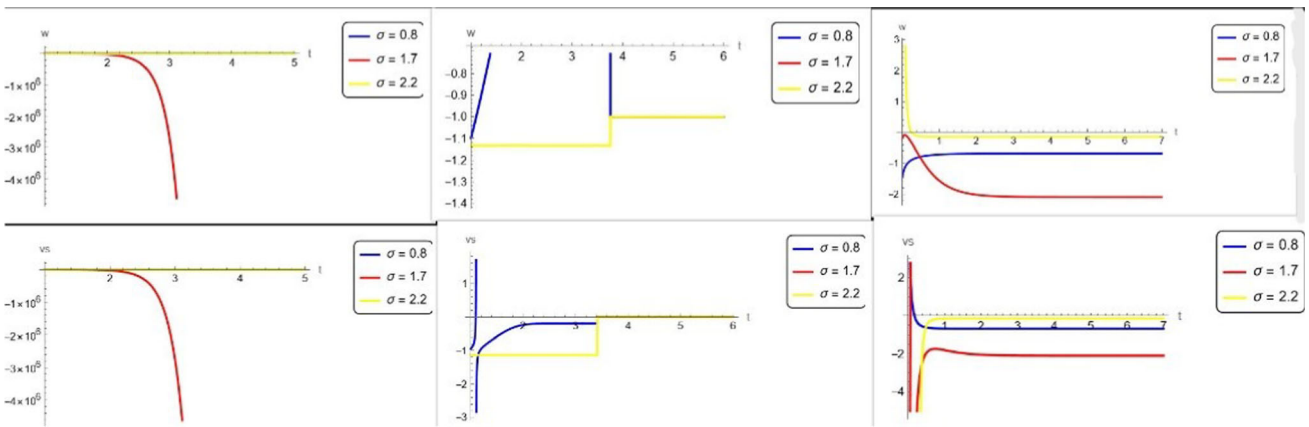


Fig. 14 Plots of the dark energy EOS parameter and squared sound speed for both LR ansatz and PR in the Tsallis paradigm. The upper panel shows the EOS parameter and the lower panel shows the squared sound speed, going from LR 1 to LR 2 to PR from left to right, in the linear interaction regime

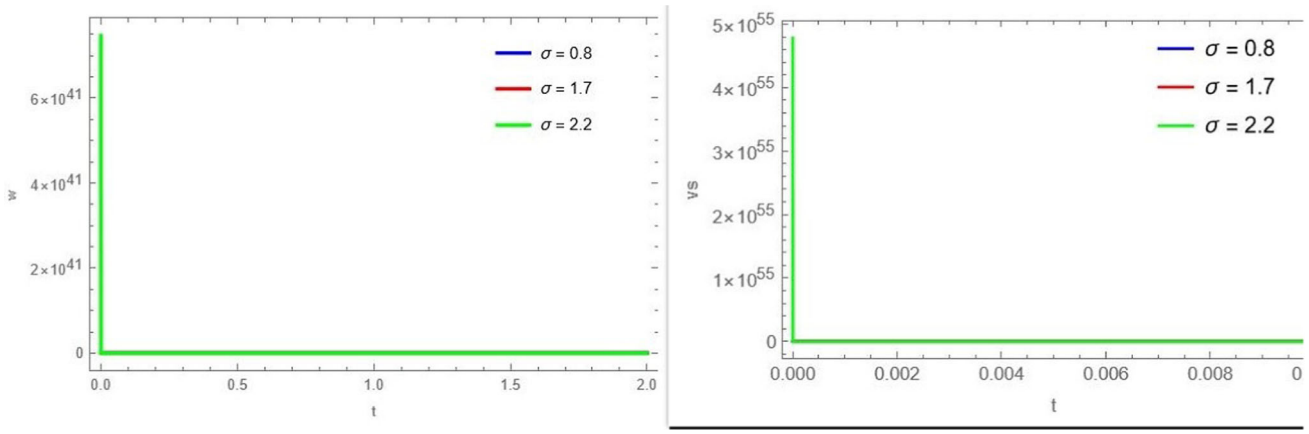


Fig. 15 Plots of dark energy EOS parameter and squared sound speed against time in the linear interaction for the Braneworld Little rip case in the Tsallis scenario

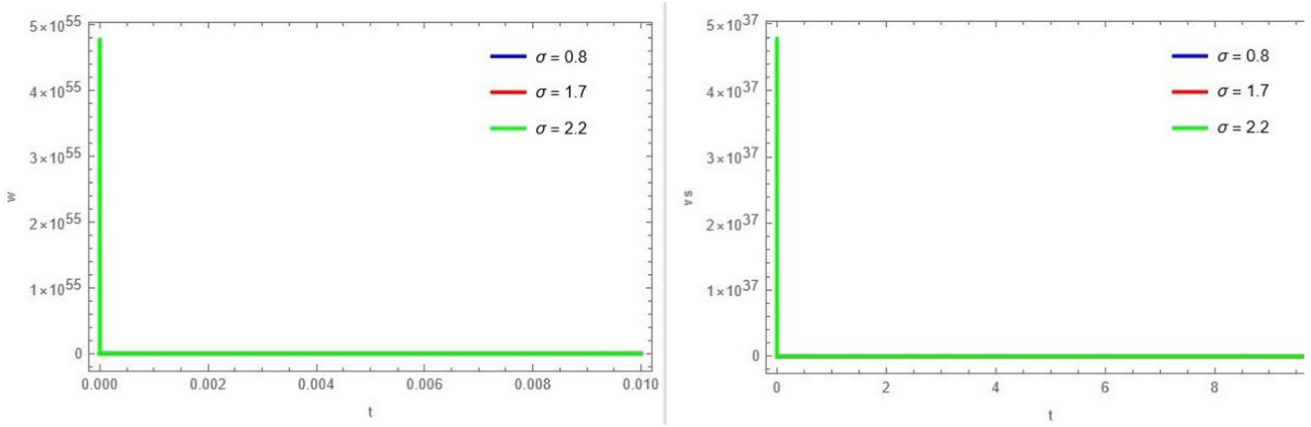


Fig. 16 Plots of dark energy EOS parameter and squared sound speed against time in the non-linear interaction for the Braneworld Little rip case in the Tsallis scenario

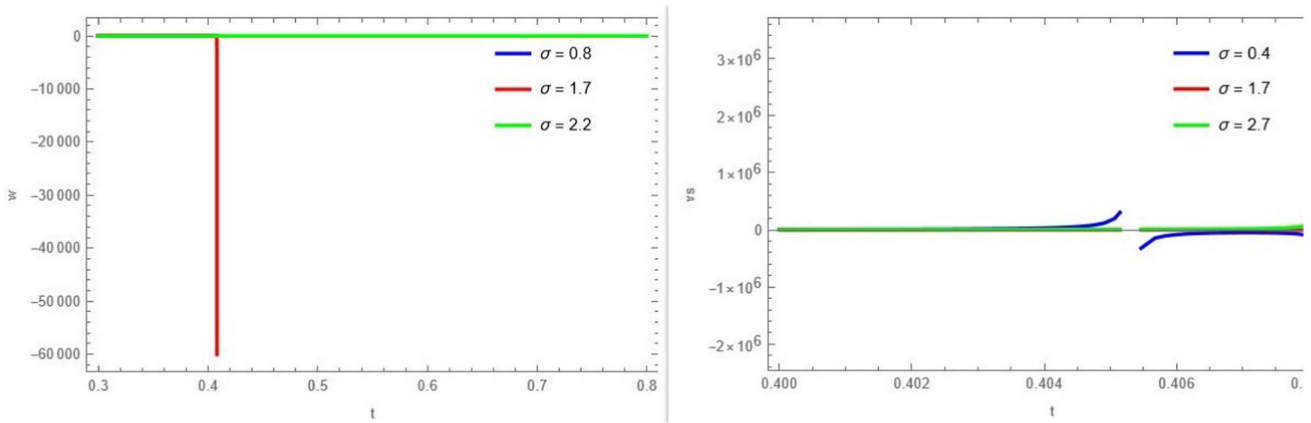


Fig. 17 Plots of dark energy EOS parameter and squared sound speed against time in the linear interaction for the Braneworld Big Freeze case in the Tsallis scenario

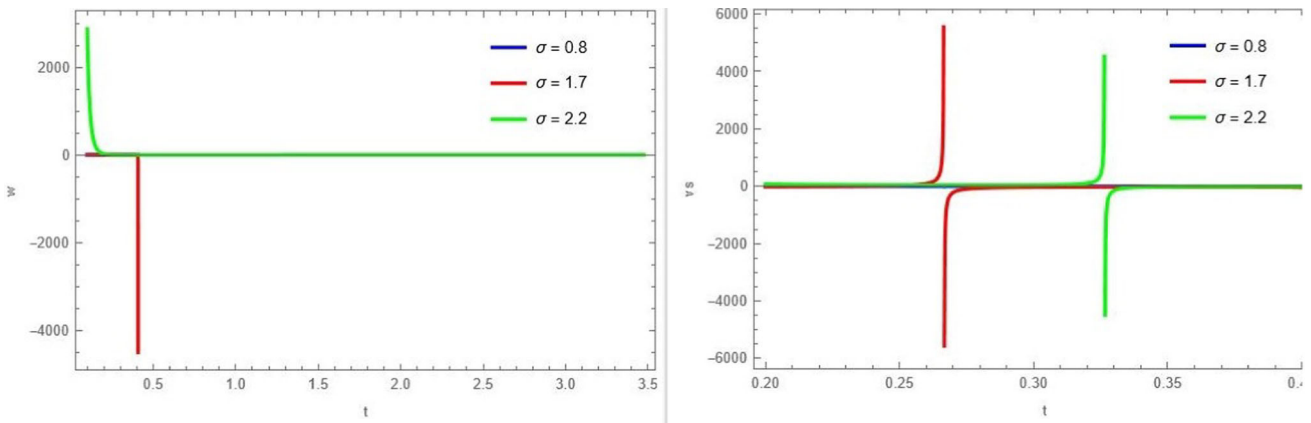


Fig. 18 Plots of dark energy EOS parameter and squared sound speed against time in the non-linear interaction for the Braneworld Big Freeze case in the Tsallis scenario

apparent horizon, with the radius [97] given by:

$$r_h = \left(H^2 + \frac{k}{a^2}\right)^{-1/2} \tag{63}$$

For a flat universe ($k = 0$), this simplifies to:

$$r_h = \frac{1}{H} \tag{64}$$

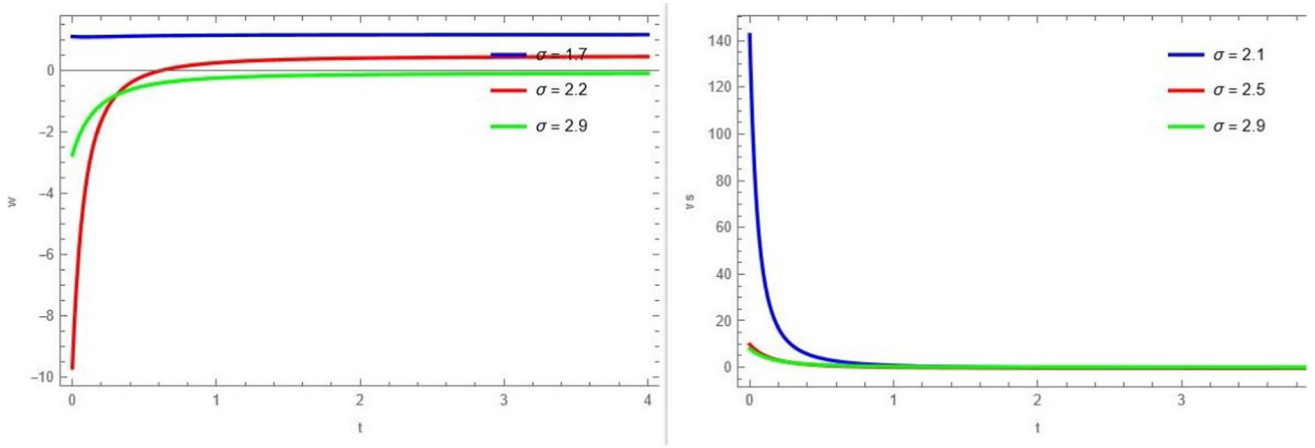


Fig. 19 Plots of dark energy EOS parameter and squared sound speed against time in the linear interaction for the Braneworld Asymptotic dS case in the Tsallis scenario

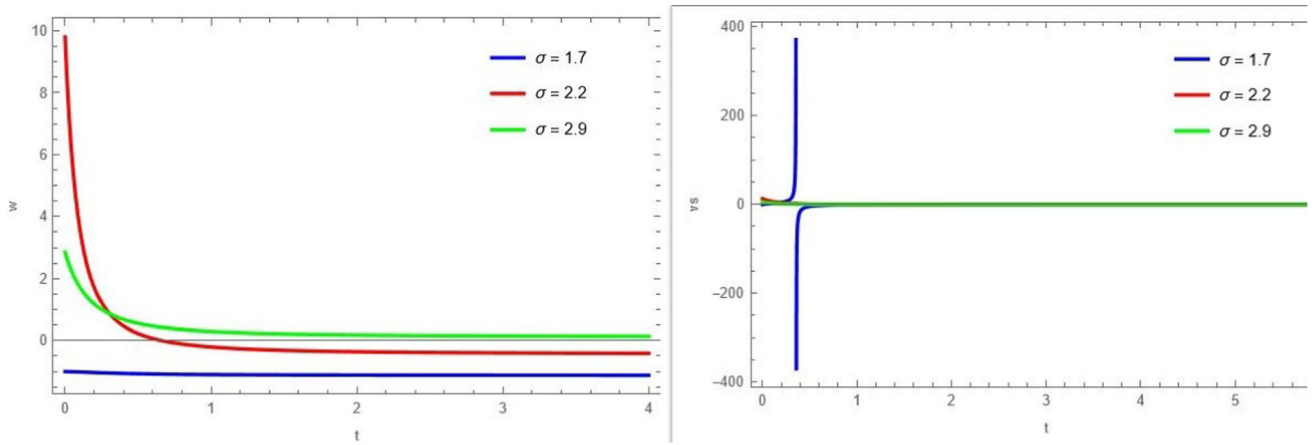


Fig. 20 Plots of dark energy EOS parameter and squared sound speed against time in the non-linear interaction for the Braneworld Asymptotic dS case in the Tsallis scenario

Considering that the major contributions to the entropy of the universe come from the dark sectors in addition to the cosmological horizon, we can write:

$$S_{tot} = S_\Lambda + S_m + S_h \tag{65}$$

where S_h is the horizon entropy. The time evolution of S_Λ and S_m can be expressed using the first law of thermodynamics as follows:

$$T\dot{S}_\Lambda = \dot{E}_\Lambda + p_\Lambda \dot{V} \tag{66}$$

$$T\dot{S}_m = \dot{E}_m + p_m \dot{V} \tag{67}$$

where $V = \frac{4\pi r_h^3}{3}$ is the horizon volume, with

$$E_\Lambda = \frac{4\pi r_h^3 \rho_\Lambda}{3}$$

and

$$E_m = \frac{4\pi r_h^3 \rho_m}{3}$$

The time evolutions of the energy densities are given by the continuity equations (33) and (34). The temperature T of the apparent horizon is given by [7]

$$T = \frac{1}{2\pi r_h} = \frac{H}{2\pi} \tag{68}$$

The entropy of the horizon depends on the HDE model we consider. In the case of the simple HDE, we use the usual Bekenstein–Hawking entropy, which can be written as:

$$S_h = \frac{A}{A_0} \tag{69}$$

[7] We have considered the Gibbons–Hawking temperature here for the cosmological apparent horizon. This has been a consideration which has been prevalent in studies of the thermodynamics of HDE before as well, see for example [96,98]. This temperature is indeed apt for a dS epoch and this consideration is fine in our study as we are interested in the properties of the very late universe here, which evolves towards an dS space with equilibrium conditions intact.

where $A_0 = \frac{1}{4G}$ is the Planck area, and we can rewrite this as:

$$S_h = \gamma r_h^2 \tag{70}$$

Here, γ is a positive constant (in this case equal to π/G, but the utility of this expression for S_h will soon be clear). When considering Barrow entropy, we have:

$$S_h = \left(\frac{A}{A_0}\right)^{1+\Delta/2} \tag{71}$$

Using the horizon radius, this can be expressed as:

$$S_h = \gamma_b r_h^{2+\Delta} \tag{72}$$

where

$$\gamma_b = \left(\frac{4\pi}{A_0}\right)^{1+\Delta/2}$$

is a positive constant. For the Tsallis HDE scenario, the horizon entropy is given by:

$$S_h = \gamma_t r_h^{2\sigma} \tag{73}$$

where γ_t is again a constant in terms of the Planck area and the Tsallis parameter. We can write the derivative of the total entropy of the universe in the case of the Hubble horizon cutoff in the conventional HDE model as

$$\dot{S} = \frac{2\pi}{H}\left[\frac{8\pi\dot{H}\Omega_d}{H} - \frac{24\pi\dot{H}}{H} - 4\pi\left(\frac{Q}{3H^2} + 3H\Omega_m(1+w_m)\right)\right] - \frac{2\gamma\dot{H}}{H^3} \tag{74}$$

Similarly we can write for the Barrow and Tsallis cases as

$$\dot{S} = \frac{2\pi}{H}\left[\frac{4\pi\dot{H}\Omega_d(2-\Delta)}{H} - \frac{24\pi\dot{H}}{H} - 4\pi\left(\frac{Q}{3H^2} + 3H\Omega_m(1+w_m)\right)\right] - \frac{(2+\Delta)\gamma_b\dot{H}}{H^2H^{1+\Delta}} \tag{75}$$

$$\dot{S} = \frac{2\pi}{H}\left[\frac{4\pi\dot{H}\Omega_d(4-2\sigma)}{H} - \frac{24\pi\dot{H}}{H} - 4\pi\left(\frac{Q}{3H^2} + 3H\Omega_m(1+w_m)\right)\right] - \frac{2\gamma_t\sigma\dot{H}}{H^2H^{2\sigma-1}} \tag{76}$$

Similarly we can find the entropy for the event horizon cases for the conventional, Tsallis and Barrow models as

$$\dot{S} = \frac{2\pi}{H}\left[8\pi\Omega_d\left(\frac{\sqrt{\Omega_d}}{c} - 1\right) - \frac{24\pi\dot{H}}{H} - 4\pi\left(\frac{Q}{3H^2} + 3H\Omega_m(1+w_m)\right)\right] - \frac{2\gamma\dot{H}}{H^3} \tag{77}$$

$$\dot{S} = \frac{2\pi}{H}\left[\frac{4\pi\Omega_d}{H}(4-2\sigma)\left(\left(\frac{\Omega_d H^2}{c^2}\right)^{\left(\frac{1}{4-2\sigma}\right)} - H\right) - \frac{24\pi\dot{H}}{H} - 4\pi\left(\frac{Q}{3H^2} + 3H\Omega_m(1+w_m)\right)\right] - \frac{2\gamma_t\sigma\dot{H}}{H^2H^{2\sigma-1}} \tag{78}$$

$$\dot{S} = \frac{2\pi}{H}\left[\frac{4\pi\Omega_d}{H}(2-\Delta)\left(\left(\frac{\Omega_d H^2}{c^2}\right)^{\left(\frac{1}{2-\Delta}\right)} - H\right) - \frac{24\pi\dot{H}}{H} - 4\pi\left(\frac{Q}{3H^2} + 3H\Omega_m(1+w_m)\right)\right] - \frac{(2+\Delta)\gamma_b\dot{H}}{H^2H^{1+\Delta}} \tag{79}$$

While we can also find it for the particle horizon case, we will not be seeing the viability of the GSL for this cutoff as we really only have one model (Tsallis with $\sigma > 2$) to talk about here. We need not plot the evolution of the entropy for every case we have, but we will at least try to get a gist of things here.

In Fig. 21 we have plotted the time derivative of the entropy for both Hubble and event horizon cutoffs and for dust and non-dust forms of dark matter with the first LR ansatz. Note that in the formulations above, the form of dark matter has not been set a priori to simple dust like $w_m = 0$ and so it would be interesting to see whether not dust like approximations make a difference too. We see that the interaction schemes or the form of dark matter is not impacting the conclusions in any case, which is conclusively that the generalized second law of thermodynamics is not held in any case.

In Fig. 21 we have plotted for the Hubble and event horizon cutoffs for LR and PR with us again seeing that in the majority of the cases there is no hope for the generalized second law to be satisfied. However, for the PR ansatz with event horizon cutoff (lower right panel) the GSL is satisfied.

We have plotted for the Braneworld case in Fig. 23 with the LR for both the cutoffs and the law is not satisfied. Similar themes were observed for the Big Freeze and Asymptotic dS cases which we have not shown here.

In Figs. 24 and 25 we have plotted the same for both usual LR ansatz and the Braneworld one as well, for the Tsallis case with event horizon and Barrow with Hubble horizon. We see that in the Braneworld and at least one non-Braneworld ansatz, the Tsallis model gives GSL consistent results while the Barrow model with Hubble horizon is not giving any optimistic results. This further reinforces the notion that the Hubble horizon is not well suited at all as a cutoff scheme for the late universe. It is indeed problematic that we are observing negative values for the derivative of the entropy and that is what we wanted to emphasize as well. For exam-

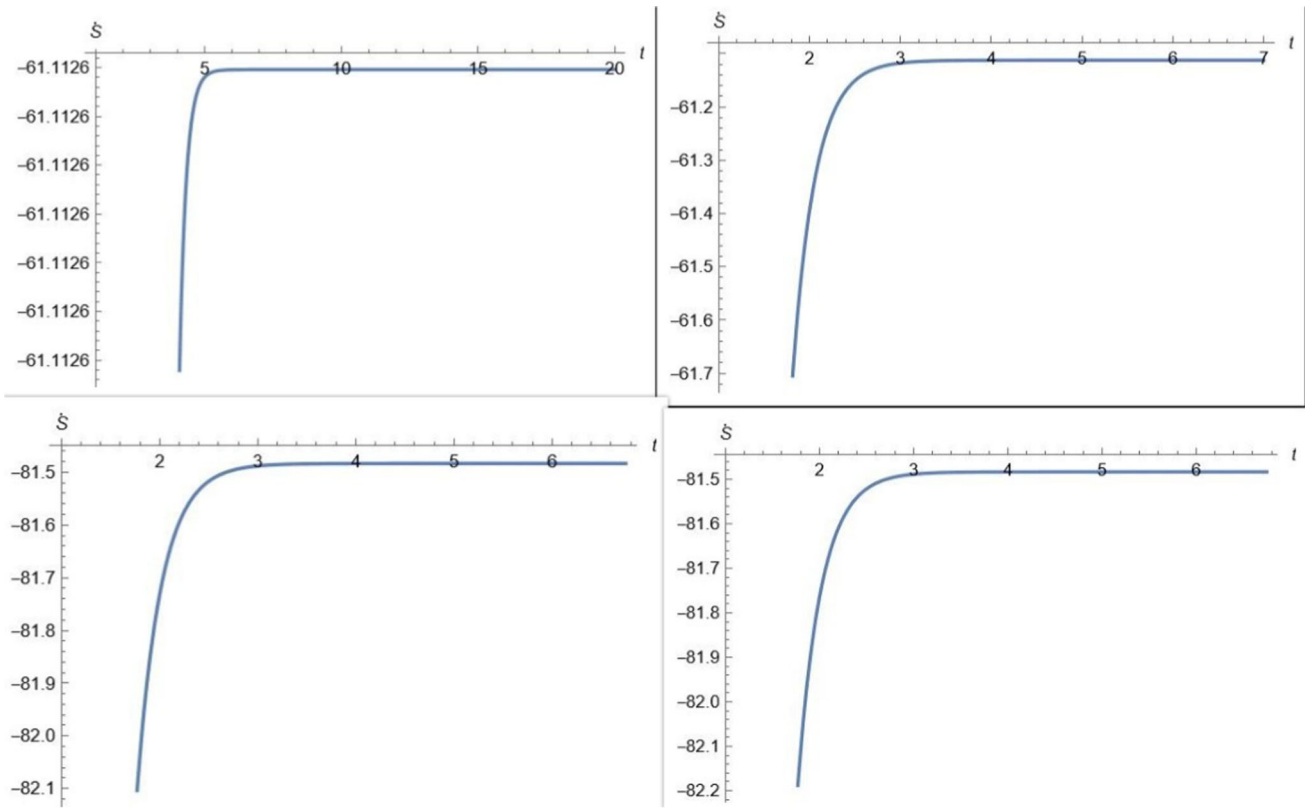


Fig. 21 Plots of the derivative of the entropy for the Hubble horizon case with first ansatz of LR. From left to right are the plots for the Hubble and Event horizon cutoffs, with upper panel for $w_m = 0$ and lower for $w_m = 1/3$

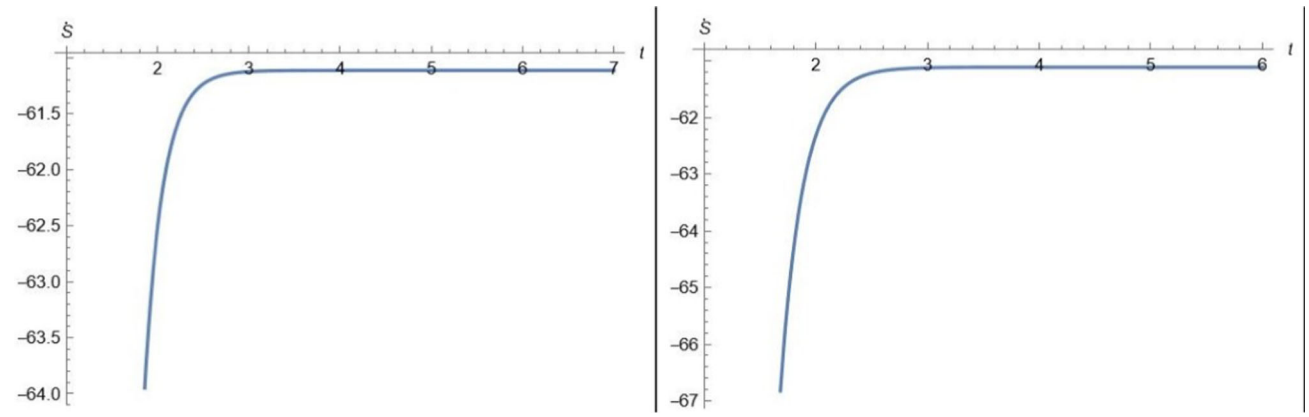


Fig. 22 Plots of the derivative of the entropy for the Hubble and event horizon cases for second LR ansatz and PR. From left to right is from Hubble horizon to event horizon cutoff, with upper panel having LR and lower panel PR

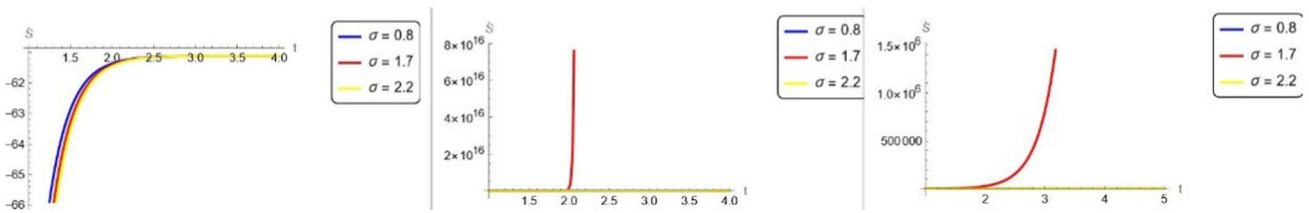


Fig. 23 Plots of the derivative of the entropy for the Hubble and event horizon cases for the LR ansatz in the Braneworld

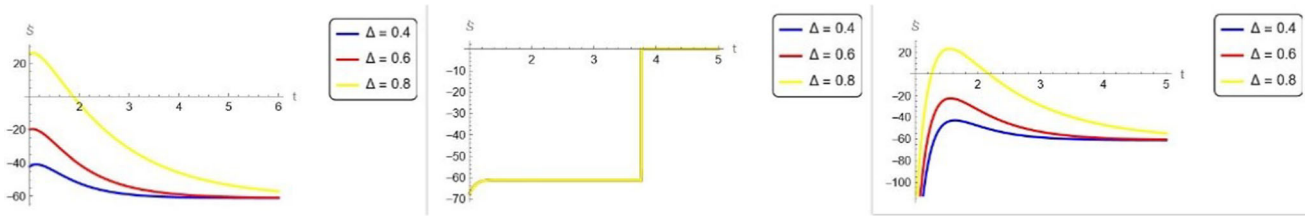


Fig. 24 Plots of the derivative of the entropy for the event horizon cutoff for both non-Braneworld and Braneworld ansatz for the Tsallis case, from left to right respectively

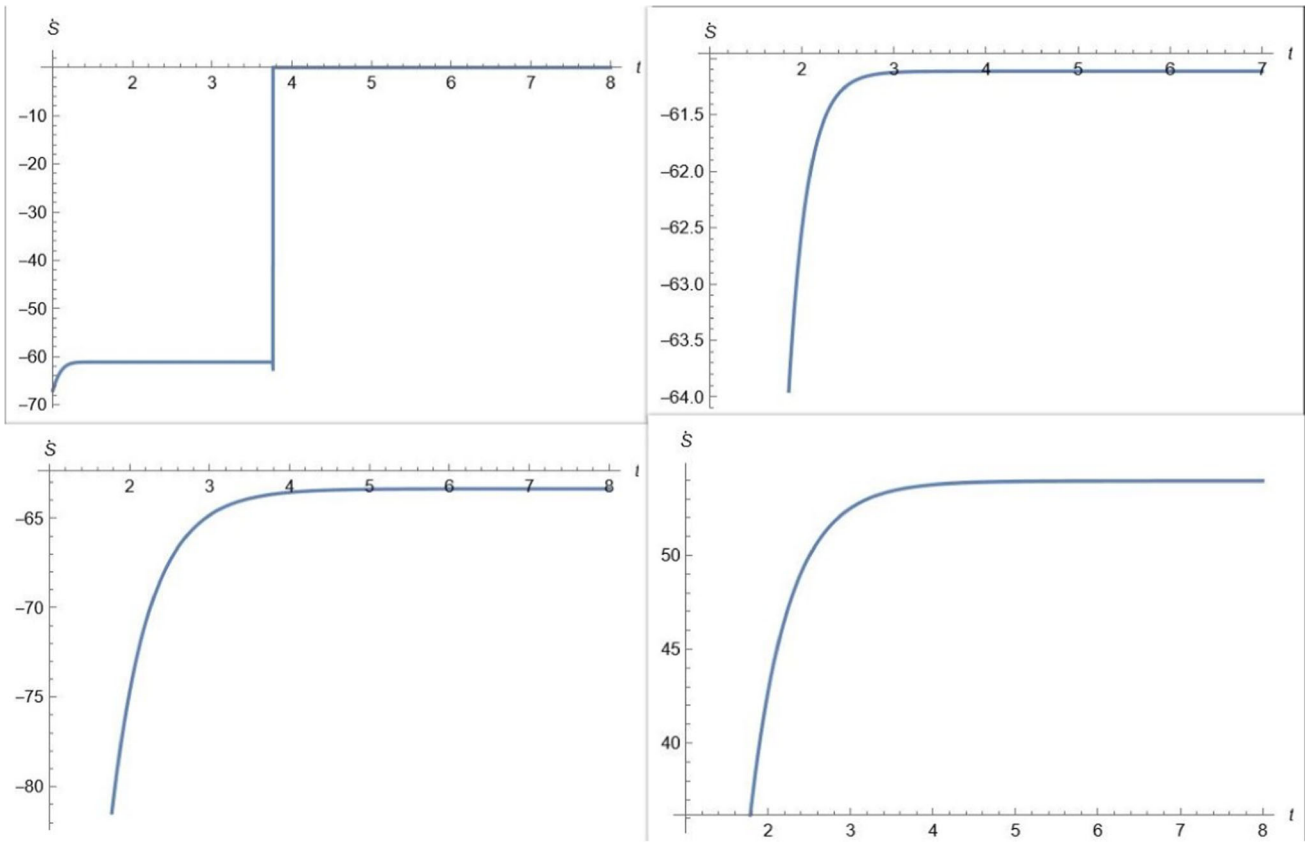


Fig. 25 Plots of the derivative of the entropy for the Hubble horizon cutoff for both non-Braneworld and Braneworld ansatz for the Barrow case, from left to right respectively

ple, in Figs. 21 and 22, where one sees negative values of the entropy derivative for cases of Little and Pseudo rip in both standard GR and Braneworld case, the plots are here to further reinforce the idea that these rip scenarios are not very sustainable and not technically possible in these HDE models. Only in very particular parameter regions, for some particular models like one seen in Fig. 24 could one have these rip scenarios to be consistent from the perspective of the second law of thermodynamics. But even when they are consistent from that perspective, they may not be consistent from the perspectives of stability, energy conditions etc. We would also like to note that there has been significant work on cosmological scenarios with such negative entropy evolution, see for example [99].

Besides these, another point of technical consistency for cosmological models can pertain to the validity of energy conditions. Four prominent energy conditions in this regard are:

- null energy condition: $p + \rho \geq 0$
- weak energy condition: $\rho \geq 0$, $\rho + p \geq 0$
- dominant energy condition: $\rho - p \geq 0$
- strong energy condition: $\rho + 3p \geq 0$

We would also like to briefly discuss the status quo of these conditions for dark energy sector in the models we have hence considered. In the case of the Hubble horizon cutoff, noting that $\rho(1+w) = p+\rho$, we can write

$$p+\rho = -H\left[\frac{Q}{3H^2} + \frac{2\dot{H}\Omega_d}{H}\right] \tag{80}$$

From the above equation, it is evident that weak and null energy conditions will be violated for all future events we have discussed here. Similarly, the strong energy condition is also violated, but for the dominant energy condition we have

$$\rho - p = 3H^2\Omega_d\left(2 + \frac{1}{3H\Omega_d}\left(\frac{Q}{3H^2} + \frac{2\dot{H}\Omega_d}{H}\right)\right) \tag{81}$$

So the dominant energy condition would hold. Similar conclusions hold true for the Barrow and the Tsallis models with this cutoff as well. Note that there is a catch here, as in the case when the Q term on right hand side of the continuity equation is positive in sign there is a possibility that all energy conditions may be satisfied. This would mean that there is a better possibility of energy conditions being satisfied if the interacting dark sector is one with DE slowly transitioning to DE instead of the other way around as of here. In the case of the particle horizon, we have only considered the Tsallis models with $\sigma > 2$, and in this scenario we can write

$$p+\rho = H\left[(4-2\sigma)\Omega_d\left(H + \left(\frac{\Omega_d H^2}{c^2}\right)^{\frac{1}{4-2\sigma}}\right) - \frac{Q}{3H^2}\right] \tag{82}$$

For the case of $\sigma > 2$, we see that the weak and null energy conditions would immediately not be satisfied and similarly not would be the strong energy condition. For the dominant energy condition we have

$$\rho - p = 3H^2\Omega_d\left(2 - \frac{1}{3H\Omega_d}(4-2\sigma)\Omega_d \times \left(H + \left(\frac{\Omega_d H^2}{c^2}\right)^{\frac{1}{4-2\sigma}}\right) - \frac{Q}{3H^2}\right) \tag{83}$$

For $\sigma > 2$ it is apparent that the dominant energy condition would be satisfied at least, again. For the event horizon case, one can not make such clear statements without plots. If we take the case of only the conventional HDE model with the event horizon cutoff, we have

$$\rho + p = H\left[2\Omega_d H\left(1 - \frac{\sqrt{\Omega_d}}{c}\right) - \frac{Q}{3H^2}\right] \tag{84}$$

$$\rho - p = 2 + \frac{1}{3H\Omega_d}\left[2\Omega_d H\left(1 - \frac{\sqrt{\Omega_d}}{c}\right) - \frac{Q}{3H^2}\right] \tag{85}$$

As is clear from the expressions above, in order to make any definitive claims about the status of the energy conditions in this case we would have to plot out these expressions for various choices of the Hubble parameter as per the events we want to consider and we currently do not pursue it here.

8 Conclusions

In this work we have discussed about the intricacies of various possible future scenarios for the universe with holographic dark energy. We started by a brief overview of various holographic dark energy models and cutoffs, alongside brief notes on rips and similar future events. We then firstly discussed about the possibility of accommodating various rip scenarios in the general N–O cutoff for HDEs, showing that the feasibility of all rip scenarios (or no rip scenario at all) is very easy to realize in the general cutoff scheme. We then turned our attention to the three primitive cutoffs for HDEs, with those being the Hubble, particle and event horizon cutoffs. We discussed in detail about rips in all of these cutoffs, considering the usual HDE model alongside the Tsallis and Barrow models in our work too. We were able to then conclude that in most cases, it is indeed rather rather hard to realize these rip scenarios both from an observational point of view and also from the view of classical stability of these regimes. We finally also discussed about the validity of various energy conditions and the generalized second law of thermodynamic in these models. We ended up showing how in general only the dominant energy condition is valid in these cases while, we did test for the weak, null and strong energy conditions too. We also showed that even the generalized second law of thermodynamics maybe violated in quite a few scenarios for these primitive cutoffs.

In passing we would also like to note that indeed in general we would not like such singularities or rips in cosmologies, but it is well discussed in the literature that for simple cutoffs like particle/event horizon a big rip singularity in general occurs in HDE models. Even further beyond that in recent work with the Granda–Oliveros cutoff [56], the point of big rips being the overarching possibility for HDE models was presented very rigorously and strongly. So the question then presented itself was that if the big rip is a possibility in general, can we avoid the big rip or at least have any of its alternatives occurring consistently ? This is an interesting question and it is vital to know which cutoff would allow for big rip alternatives as well, as that would show that the particular cutoff is perhaps the best one. Again, we see that simple cutoffs like Hubble horizon,event horizon etc. do not allow for any big rip alternatives in general from various standpoints in this work. This goes to show how even though these cutoffs are a form of N–O cutoff, they are yet just very special cases while N–O cutoffs in general accommodate a lot more freedom and bigger cosmic evolution paradigms than them. Furthermore, we studied these future events in all of these cutoffs

under these three HDE forms (conventional, Tsallis and Barrow) because we wanted to have a conclusive and definitive answer to which future events such cutoffs can realistically allow for or not. We wanted to test them out for these scenarios from an observational standpoint (EOS parameters) and also from theoretical standpoints (validity of generalized second law, energy conditions, squared sound speed). By studying these models and seeing which future possibilities are allowed for, we wanted to show just how much more generality the NO cutoff encapsulates when compared to any other cutoff scheme. The work seems to reinforce the notion more clearly that even though all the cutoffs are just special forms of the N–O cutoff, the difference in the range of possibilities which can be accommodated in the general cutoff as compared to the other ones is indeed very big.

Acknowledgements The work of S.D.O was partially supported by MICINN (Spain), project PID2019-104397GB-I00 and by the program Unidad de Excelencia Maria de Maeztu CEX2020-001058-M, Spain. The research by M.K. was carried out at Southern Federal University with financial support from the Ministry of Science and Higher Education of the Russian Federation (State contract GZ0110/23-10-IF). The authors would also like to thank Robert Scherrer for various helpful discussions.

Data Availability Statement This manuscript has no associated data. [Authors' comment: Data sharing not applicable to this article as no datasets were generated or analysed during the current study.]

Code Availability Statement This manuscript has no associated code/software. [Authors' comment: Code/Software sharing not applicable to this article as no code/software was generated or analysed during the current study.]

Open Access This article is licensed under a Creative Commons Attribution 4.0 International License, which permits use, sharing, adaptation, distribution and reproduction in any medium or format, as long as you give appropriate credit to the original author(s) and the source, provide a link to the Creative Commons licence, and indicate if changes were made. The images or other third party material in this article are included in the article's Creative Commons licence, unless indicated otherwise in a credit line to the material. If material is not included in the article's Creative Commons licence and your intended use is not permitted by statutory regulation or exceeds the permitted use, you will need to obtain permission directly from the copyright holder. To view a copy of this licence, visit http://creativecommons.org/licenses/by/4.0/.
Funded by SCOAP[3].

References

1. A.G. Riess et al., Observational evidence from supernovae for an accelerating universe and a cosmological constant. Astron. J. **116**, 1009–1038 (1998). https://doi.org/10.1086/300499. arXiv:astro-ph/9805201
2. S. Weinberg, The cosmological constant problem. Rev. Mod. Phys. **61**, 1–23 (1989). https://doi.org/10.1103/RevModPhys.61.1
3. L. Lombriser, On the cosmological constant problem. Phys. Lett. B **797**, 134804 (2019). https://doi.org/10.1016/j.physletb.2019.134804. arXiv:1901.08588 [gr-qc]
4. T. Padmanabhan, Cosmological constant: the weight of the vacuum. Phys. Rep. **380**, 235–320 (2003). https://doi.org/10.1016/S0370-1573(03)00120-0. arXiv:hep-th/0212290
5. S. Capozziello, M. De Laurentis, Extended theories of gravity. Phys. Rep. **509**, 167–321 (2011). https://doi.org/10.1016/j.physrep.2011.09.003. arXiv:1108.6266 [gr-qc]
6. S. Nojiri, S.D. Odintsov, Unified cosmic history in modified gravity: from F(R) theory to Lorentz non-invariant models. Phys. Rep. **505**, 59–144 (2011). https://doi.org/10.1016/j.physrep.2011.04.001. arXiv:1011.0544 [gr-qc]
7. S. Nojiri, S.D. Odintsov, V.K. Oikonomou, Modified gravity theories on a nutshell: inflation, bounce and late-time evolution. Phys. Rep. **692**, 1–104 (2017). https://doi.org/10.1016/j.physrep.2017.06.001. arXiv:1705.11098 [gr-qc]
8. I. Zlatev, L.-M. Wang, P.J. Steinhardt, Quintessence, cosmic coincidence, and the cosmological constant. Phys. Rev. Lett. **82**, 896–899 (1999). https://doi.org/10.1103/PhysRevLett.82.896. arXiv:astro-ph/9807002
9. V. Faraoni, Inflation and quintessence with nonminimal coupling. Phys. Rev. D **62**, 023504 (2000). https://doi.org/10.1103/PhysRevD.62.023504. arXiv:gr-qc/0002091
10. M. Gasperini, F. Piazza, G. Veneziano, Quintessence as a runaway dilaton. Phys. Rev. D **65**, 023508 (2002). https://doi.org/10.1103/PhysRevD.65.023508. arXiv:gr-qc/0108016
11. S. Capozziello, S. Carloni, A. Troisi, Quintessence without scalar fields. Recent Res. Dev. Astron. Astrophys. **1**, 625 (2003). arXiv:astro-ph/0303041
12. S. Capozziello, Curvature quintessence. Int. J. Mod. Phys. D **11**, 483–492 (2002). https://doi.org/10.1142/S0218271802002025. arXiv:gr-qc/0201033
13. S.D. Odintsov et al., Recent advances on inflation. Symmetry **15**, 9 (2023). https://doi.org/10.3390/sym15091701. arXiv:2307.16308 [gr-qc]
14. V. Sahni, Y. Shtanov, Brane world models of dark energy. JCAP **11**, 014 (2003). https://doi.org/10.1088/1475-7516/2003/11/014. arXiv:astro-ph/0202346
15. M. Sami, V. Sahni, Quintessential inflation on the brane and the relic gravity wave background. Phys. Rev. D **70**, 083513 (2004). https://doi.org/10.1103/PhysRevD.70.083513. arXiv:hep-th/0402086
16. P. Tretyakov et al., Quantum effects, soft singularities and the fate of the universe in a braneworld cosmology. Class. Quantum Gravity **23**, 3259–3274 (2006). https://doi.org/10.1088/0264-9381/23/10/001. arXiv:gr-qc/0510104
17. S. Chen, B. Wang, J. Jing, Dynamics of interacting dark energy model in Einstein and Loop Quantum Cosmology. Phys. Rev. D **78**, 123503 (2008). https://doi.org/10.1103/PhysRevD.78.123503. arXiv:0808.3482 [gr-qc]
18. F. Xiangyun, Yu. Hong Wei, W. Puxun, Dynamics of interacting phantom scalar field dark energy in Loop Quantum Cosmology. Phys. Rev. D **78**, 063001 (2008). https://doi.org/10.1103/PhysRevD.78.063001. arXiv:0808.1382 [gr-qc]
19. A. Bonanno, M. Reuter, Cosmology with selfadjusting vacuum energy density from a renormalization group fixed point. Phys. Lett. B **527**, 9–17 (2002). https://doi.org/10.1016/S0370-2693(01)01522-2. arXiv:astro-ph/0106468
20. A. Bonanno, M. Reuter, Cosmology of the Planck era from a renormalization group for quantum gravity. Phys. Rev. D **65**, 043508 (2002). https://doi.org/10.1103/PhysRevD.65.043508. arXiv:hep-th/0106133
21. E. Bentivegna, A. Bonanno, M. Reuter, Confronting the IR fixed point cosmology with high redshift supernova data. JCAP **01**, 001 (2004). https://doi.org/10.1088/1475-7516/2004/01/001. arXiv:astro-ph/0303150
22. M. Reuter, F. Saueressig, From big bang to asymptotic de Sitter: complete cosmologies in a quantum gravity framework. JCAP

09, 012 (2005). https://doi.org/10.1088/1475-7516/2005/09/012. arXiv:hep-th/0507167
23. A. Bonanno, M. Reuter, Entropy signature of the running cosmological constant. JCAP **08**, 024 (2007). https://doi.org/10.1088/1475-7516/2007/08/024. arXiv:0706.0174 [hep-th]
24. S. Weinberg, Asymptotically safe inflation. Phys. Rev. D **81**, 083535 (2010). https://doi.org/10.1103/PhysRevD.81.083535. arXiv:0911.3165 [hep-th]
25. Planck Collaboration, N. Aghanim et al., Planck 2018 results. VI. Cosmological parameters. Astron. Astrophys. 641, A6 (2020) [Erratum: Astron. Astrophys. 652, C4 (2021)]. https://doi.org/10.1051/0004-6361/201833910. arXiv:1807.06209 [astro-ph.CO]
26. A.G. Riess et al., Large Magellanic Cloud Cepheid standards provide a 1% foundation for the determination of the Hubble constant and stronger evidence for physics beyond MathID1CDM. Astrophys. J. **876**(1), 85 (2019)
27. A.G. Riess et al., A comprehensive measurement of the local value of the Hubble constant with 1 km/s/Mpc uncertainty from the Hubble Space Telescope and the SH0ES Team. arXiv preprint arXiv:2112.04510 (2021)
28. G. 't Hooft, Dimensional reduction in quantum gravity. Conf. Proc. C **930308**, 284–296 (1993). arXiv:gr-qc/9310026
29. L. Susskind, The world as a hologram. J. Math. Phys. **36**, 6377–6396 (1995). https://doi.org/10.1063/1.531249. arXiv:hep-th/9409089
30. R. Bousso, A covariant entropy conjecture. JHEP **07**, 004 (1999). https://doi.org/10.1088/1126-6708/1999/07/004. arXiv:hep-th/9905177
31. A.G. Adame et al., DESI 2024 IV: baryon acoustic oscillations from the Lyman Alpha Forest. (2024). arXiv:2404.03001 [astro-ph.CO]
32. A.G. Adame et al., DESI 2024 VI: cosmological constraints from the measurements of baryon acoustic oscillations (2024). arXiv:2404.03002 [astro-ph.CO]
33. A.G. Adame et al., DESI 2024 III: baryon acoustic oscillations from galaxies and quasars (2024). arXiv:2404.03000 [astro-ph.CO]
34. A.G. Cohen, D.B. Kaplan, A.E. Nelson, Effective field theory, black holes, and the cosmological constant. Phys. Rev. Lett. **82**, 4971–4974 (1999). https://doi.org/10.1103/PhysRevLett.82.4971. arXiv:hep-th/9803132
35. S. Wang, Y. Wang, M. Li, Holographic dark energy. Phys. Rep. **696**, 1–57 (2017). https://doi.org/10.1016/j.physrep.2017.06.003. arXiv:1612.00345 [astro-ph.CO]
36. S. Nojiri, S.D. Odintsov, Covariant generalized holographic dark energy and accelerating universe. Eur. Phys. J. C **77**(8), 528 (2017). https://doi.org/10.1140/epjc/s10052-017-5097-x. arXiv:1703.06372 [hep-th]
37. A. Oliveros, M.A. Sabogal, M.A. Acero, Barrow holographic dark energy with Granda–Oliveros cutoff. Eur. Phys. J. Plus **137**(7), 783 (2022). https://doi.org/10.1140/epjp/s13360-022-02994-z. arXiv:2203.14464 [gr-qc]
38. L.N. Granda, A. Oliveros, Infrared cut-off proposal for the Holographic density. Phys. Lett. B **669**, 275–277 (2008). https://doi.org/10.1016/j.physletb.2008.10.017. arXiv:0810.3149 [gr-qc]
39. M. Khurshudyan, Viscous holographic dark energy universe with Nojiri–Odintsov cut-off. Astrophys. Space Sci. **361**(12), 392 (2016). https://doi.org/10.1007/s10509-016-2981-z
40. M. Khurshudyan, On a holographic dark energy model with a Nojiri–Odintsov cut-off in general relativity. Astrophys. Space Sci. **361**(7), 232 (2016). https://doi.org/10.1007/s10509-016-2821-1. arXiv:1606.05264 [gr-qc]
41. M.-H. Belkacemi et al., The holographic induced gravity model with a Ricci dark energy: smoothing the little rip and big rip through Gauss–Bonnet effects? Phys. Rev. D **85**, 083503 (2012). https://doi.org/10.1103/PhysRevD.85.083503. arXiv:1112.5836 [gr-qc]
42. L. Zhang, W. Puxun, Yu. Hongwei, Unifying dark energy and dark matter with the modified Ricci model. Eur. Phys. J. C **71**, 1588 (2011). https://doi.org/10.1140/epjc/s10052-011-1588-3
43. M.R. Setare, M. Jamil, Statefinder diagnostic and stability of modified gravity consistent with holographic and new agegraphic dark energy. Gen. Relativ. Gravit. **43**, 293–303 (2011). https://doi.org/10.1007/s10714-010-1087-0. arXiv:1008.4763 [gr-qc]
44. K. Nozari, N. Rashidi, Holographic dark energy from a modified GBIG scenario. Int. J. Mod. Phys. D **19**, 219–231 (2010). https://doi.org/10.1142/S021827181001635X. arXiv:0912.4802 [gr-qc]
45. A. Sheykhi, Interacting holographic dark energy in Brans–Dicke theory. Phys. Lett. B **681**, 205–209 (2009). https://doi.org/10.1016/j.physletb.2009.10.011. arXiv:0907.5458 [hep-th]
46. X. Lixin, L. Jianbo, W. Li, Generalized holographic and Ricci dark energy models. Eur. Phys. J. C **64**, 89–95 (2009). https://doi.org/10.1140/epjc/s10052-009-1122-z. arXiv:0906.0210 [astro-ph.CO]
47. H. Wei, Modified holographic dark energy. Nucl. Phys. B **819**, 210–224 (2009). https://doi.org/10.1016/j.nuclphysb.2009.04.020. arXiv:0902.2030 [gr-qc]
48. M.R. Setare, E.N. Saridakis, Correspondence between holographic and Gauss–Bonnet dark energy models. Phys. Lett. B **670**, 1–4 (2008). https://doi.org/10.1016/j.physletb.2008.10.029. arXiv:0810.3296 [hep-th]
49. E.N. Saridakis, Holographic dark energy in braneworld models with a Gauss–Bonnet term in the bulk. Interacting behavior and the w =-1 crossing. Phys. Lett. B **661**, 335–341 (2008). https://doi.org/10.1016/j.physletb.2008.02.032. arXiv:0712.3806 [gr-qc]
50. M.R. Setare, The holographic dark energy in non-flat Brans–Dicke cosmology. Phys. Lett. B **644**, 99–103 (2007). https://doi.org/10.1016/j.physletb.2006.11.033. arXiv:hep-th/0610190
51. F. Felegary, F. Darabi, M.R. Setare, Interacting holographic dark energy model in Brans–Dicke cosmology and coincidence problem. Int. J. Mod. Phys. D **27**(03), 1850017 (2017). https://doi.org/10.1142/S0218271818500177. arXiv:1612.03406 [gr-qc]
52. M. Dheepika, T.K. Mathew, Tsallis holographic dark energy reconsidered. Eur. Phys. J. C **82**(5), 399 (2022). https://doi.org/10.1140/epjc/s10052-022-10365-2. arXiv:2110.04031 [gr-qc]
53. S. Nojiri, S.D. Odintsov, Unifying phantom inflation with late-time acceleration: scalar phantom-non-phantom transition model and generalized holographic dark energy. Gen. Relativ. Gravit. **38**, 1285–1304 (2006). https://doi.org/10.1007/s10714-006-0301-6. arXiv:hep-th/0506212
54. S. Nojiri, S.D. Odintsov, T. Paul, Different faces of generalized holographic dark energy. Symmetry **13**(6), 928 (2021). https://doi.org/10.3390/sym13060928. arXiv:2105.08438 [gr-qc]
55. S. Nojiri et al., Unifying holographic inflation with holographic dark energy: a covariant approach. Phys. Rev. D **102**(2), 023540 (2020). https://doi.org/10.1103/PhysRevD.102.023540. arXiv:2007.06829 [gr-qc]
56. O. Trivedi, R.J. Scherrer, New perspectives on future rip scenarios with holographic dark energy (2024). arXiv:2404.08912 [astro-ph.CO]
57. O. Trivedi, M. Khlopov, A.V. Timoshkin, Tsallis holographic dark energy with power law ansatz approach (2024). arXiv:2402.05784 [gr-qc]
58. M. Tavayef et al., Tsallis holographic dark energy. Phys. Lett. B **781**, 195–200 (2018). https://doi.org/10.1016/j.physletb.2018.04.001. arXiv:1804.02983 [gr-qc]
59. E.N. Saridakis, Barrow holographic dark energy. Phys. Rev. D **102**(12), 123525 (2020). https://doi.org/10.1103/PhysRevD.102.123525. arXiv:2005.04115 [gr-qc]
60. S. Nojiri, S.D. Odintsov, Quantum escape of sudden future singularity. Phys. Lett. B **595**, 1–8 (2004). https://doi.org/10.1016/j.physletb.2004.06.060. arXiv:hep-th/0405078
61. S. Nojiri, S.D. Odintsov, Inhomogeneous equation of state of the universe: phantom era, future singularity and crossing the phantom

barrier. Phys. Rev. D **72**, 023003 (2005). https://doi.org/10.1103/PhysRevD.72.023003. arXiv:hep-th/0505215
62. S. Nojiri, S.D. Odintsov, S. Tsujikawa, Properties of singularities in (phantom) dark energy universe. Phys. Rev. D **71**, 063004 (2005). https://doi.org/10.1103/PhysRevD.71.063004. arXiv:hep-th/0501025
63. K. Bamba, S. Nojiri, S.D. Odintsov, The universe future in modified gravity theories: approaching the finite-time future singularity. JCAP **10**, 045 (2008). https://doi.org/10.1088/1475-7516/2008/10/045. arXiv:0807.2575 [hep-th]
64. O. Trivedi, M. Khlopov, On finite time singularities in scalar field dark energy models based in the RS-II Braneworld. arXiv preprint arXiv:2201.01015 (2022)
65. O. Trivedi, M. Khlopov, Type V singularities in non-standard cosmological backgrounds. Phys. Dark Universe **36**, 101041 (2022)
66. S.D. Odintsov, V.K. Oikonomou, Singular inflationary universe from F (R) gravity. Phys. Rev. D **92**(12), 124024 (2015)
67. S.D. Odintsov, V.K. Oikonomou, Singular F (R) cosmology unifying early-and late-time acceleration with matter and radiation domination era. Class. Quantum Gravity **33**(12), 125029 (2016)
68. V.K. Oikonomou, Singular bouncing cosmology from Gauss–Bonnet modified gravity. Phys. Rev. D **92**(12), 124027 (2015)
69. S. Nojiri, S.D. Odintsov, V.K. Oikonomou, Singular inflation from generalized equation of state fluids. Phys. Lett. B **747**, 310–320 (2015)
70. S.D. Odintsov, V.K. Oikonomou, Did the Universe experience a pressure non-crushing type cosmological singularity in the recent past? Europhys. Lett. **137**(3), 39001 (2022)
71. O. Trivedi, A.V. Timoshkin, Little rip, pseudo rip and bounce cosmology with generalized equation of state in non-standard backgrounds (2023). arXiv:2309.05047 [gr-qc]
72. O. Trivedi et al., Cosmological singularities in MathID2 gravity. Eur. Phys. J. C **83**(11), 1017 (2023). https://doi.org/10.1140/epjc/s10052-023-12204-4. arXiv:2310.20222 [gr-qc]
73. O. Trivedi, S.K. Saggu, P.S. Joshi, Cosmological singularities in non-canonical models of dark energy. Phys. Dark Universe **42**, 101366 (2023). https://doi.org/10.1016/j.dark.2023.101366. arXiv:2310.00452 [gr-qc]
74. O. Trivedi, Recent advances in cosmological singularities (2023). arXiv:2309.08954 [gr-qc]
75. J. de Haro et al., Finite-time cosmological singularities and the possible fate of the Universe. Phys. Rep. **1034**, 1–114 (2023). https://doi.org/10.1016/j.physrep.2023.09.003. arXiv:2309.07465 [gr-qc]
76. R.R. Caldwell, M. Kamionkowski, N.N. Weinberg, Phantom energy and cosmic doomsday. Phys. Rev. Lett. **91**, 071301 (2003). https://doi.org/10.1103/PhysRevLett.91.071301. arXiv:astro-ph/0302506
77. P.H. Frampton, K.J. Ludwick, R.J. Scherrer, The little rip. Phys. Rev. D **84**, 063003 (2011). https://doi.org/10.1103/PhysRevD.84.063003. arXiv:1106.4996 [astro-ph.CO]
78. P.H. Frampton, K.J. Ludwick, R.J. Scherrer, Pseudo-rip: cosmological models intermediate between the cosmological constant and the little rip. Phys. Rev. D **85**, 083001 (2012). https://doi.org/10.1103/PhysRevD.85.083001. arXiv:1112.2964 [astro-ph.CO]
79. J.D. Barrow, Sudden future singularities. Class. Quantum Gravity **21**, L79–L82 (2004). https://doi.org/10.1088/0264-9381/21/11/L03. arXiv:gr-qc/0403084
80. L. Andersson, A.D. Rendall, Quiescent cosmological singularities. Commun. Math. Phys. **218**, 479–511 (2001). https://doi.org/10.1007/s002200100406. arXiv:gr-qc/0001047
81. V. Gorini et al., Tachyons, scalar fields and cosmology. Phys. Rev. D **69**, 123512 (2004). https://doi.org/10.1103/PhysRevD.69.123512. arXiv:hep-th/0311111
82. M. Bouhmadi-López, P.F. González-Dıaz, P. Martın-Moruno, Worse than a big rip? Phys. Lett. B **659**(1–2), 1–5 (2008)
83. S. Nojiri, S.D. Odintsov, The final state and thermodynamics of dark energy universe. Phys. Rev. D **70**, 103522 (2004). https://doi.org/10.1103/PhysRevD.70.103522. arXiv:hep-th/0408170
84. S. Nojiri, S.D. Odintsov, AdS/CFT correspondence, conformal anomaly and quantum corrected entropy bounds. Int. J. Mod. Phys. A **16**, 3273–3290 (2001). https://doi.org/10.1142/S0217751X01004128. arXiv:hep-th/0011115
85. O. Trivedi, M. Khlopov, Singularity formation in asymptotically safe cosmology with inhomogeneous equation of state. JCAP **11**, 007 (2022). https://doi.org/10.1088/1475-7516/2022/11/007. arXiv:2204.06437 [gr-qc]
86. S. Nojiri, S.D. Odintsov, The future evolution and finite-time singularities in F(R)-gravity unifying the inflation and cosmic acceleration. Phys. Rev. D **78**, 046006 (2008). https://doi.org/10.1103/PhysRevD.78.046006. arXiv:0804.3519 [hep-th]
87. J.D. Barrow, Cosmologies with varying light speed. Phys. Rev. D **59**(4), 043515 (1999)
88. M.P. Dabrowski et al., New tests of variability of the speed of light. EPJ Web Conf. **126**, 04012 (2016)
89. M.P. Dabrowski, K. Marosek, Regularizing cosmological singularities by varying physical constants. JCAP **02**, 012 (2013). https://doi.org/10.1088/1475-7516/2013/02/012. arXiv:1207.4038 [hep-th]
90. K. Leszczynska, A. Balcerzak, M.P. Dabrowski, Varying constants quantum cosmology. JCAP **02**, 012 (2015). https://doi.org/10.1088/1475-7516/2015/02/012. arXiv:1411.6094 [hep-th]
91. V. Salzano, M.P. Dabrowski, Statistical hierarchy of varying speed of light cosmologies. Astrophys. J. **851**(2), 97 (2017). https://doi.org/10.3847/1538-4357/aa9cea. arXiv:1612.06367 [astro-ph.CO]
92. R.-G. Cai et al., Notes on ghost dark energy. Phys. Rev. D **84**(12), 123501 (2011)
93. M. Li, A model of holographic dark energy. Phys. Lett. B **603**(1–2), 1–5 (2004)
94. P.H. Frampton et al., Models for little rip dark energy. Phys. Lett. B **708**, 204–211 (2012). https://doi.org/10.1016/j.physletb.2012.01.048. arXiv:1108.0067 [hep-th]
95. A.V. Astashenok, S.D. Odintsov, Confronting dark energy models mimicking MathID3CDM epoch with observational constraints: future cosmological perturbations decay or future Rip? Phys. Lett. B **718**, 1194–1202 (2013). https://doi.org/10.1016/j.physletb.2012.12.058. arXiv:1211.1888 [gr-qc]
96. A. Al Mamon, A.H. Ziaie, K. Bamba, A generalized interacting Tsallis holographic dark energy model and its thermodynamic implications. Eur. Phys. J. C **80**(10), 974 (2020). https://doi.org/10.1140/epjc/s10052-020-08546-y. arXiv:2004.01593 [gr-qc]
97. D. Bak, S.-J. Rey, Cosmic holography. Class. Quantum Gravity **17**, L83 (2000). https://doi.org/10.1088/0264-9381/17/15/101. arXiv:hep-th/9902173
98. G. Chakraborty et al., Thermodynamics of barrow holographic dark energy with specific cut-off. Symmetry **13**(4), 562 (2021). https://doi.org/10.3390/sym13040562
99. I. Brevik, Ø. Grøn, Universe models with negative bulk viscosity. Astrophys. Space Sci. **347**, 399–404 (2013)